2p(mix)

NTIS $6.50

NATIONAL AERONAUTICS AND SPACE ADMINISTRATION

EARTH RESOURCES PROGRAM

SQT

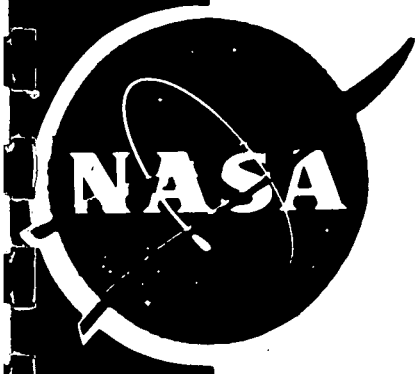

TECHNICAL REPORT 6

REMOTE SENSING EVALUATION OF THE KLONDIKE MINING DISTRICT, NEVADA

PART I - GEOLOGY, PHOTOGRAPHY and INFRARED

by

P.A. BRENNAN, P.E. CHAPMAN and E.R. CHIPP

UNIVERSITY OF NEVADA RENO
89507

CONTRACT NO. NAS9-7779

1971

TECHNICAL REPORT 6

Remote Sensing Evaluation of the Klondike Mining District, Nevada

Part I: Geology, Photography and Infrared

by

Peter A. Brennan*

Peter E. Chapman*

Eddie R. Chipp*

Contract NAS 9-7779

1971

* Peter A. Brennan, Former Research Assoc. NASA Project, University of Nevada, Presently with; Aero Service Corp. Philadelphia, PA. 19135.
* Peter E. Chapman, Former Research Assoc. NASA Project, University of Nevada, Presently with; Cyprus Mines Corp., Getchell, NV.
* Eddie R. Chipp, Former Graduate Student, University of Nevada, Presently with; Resource Associates of Alaska, Inc. Fairbanks, Alaska 99791.

TABLE OF CONTENTS

TABLE OF CONTENTS (Continued)

TABLE OF CONTENTS (Continued)

ABSTRACT

During August of 1970 Mission 140 was flown with the NASA P3A aircraft over the Klondike Mining District, Nevada. High quality metric photography, thermal infrared imagery, multispectral photography and multichannel microwave radiometry were obtained. Geology and "ground truth" data are presented and relationships of the physical attributes of geologic materials to remotely sensed data is discussed. It is concluded that remote sensing data was valuable in the geologic evaluation of the Klondike Mining District and would be of value in other mining districts.

ACKNOWLEDGEMENTS

The authors wish to acknowledge the support provided by Mr. Jack G. Quade of the National Aeronautics and Space Administration, University of Nevada Reno. Particular thanks are due to Mr. Olav Smistad and Mr. David Amsbury of NASA Houston for fostering an atmosphere conducive to such research projects and to those who have worked overtime preparing many of the plates, figures, diagrams, and typing the manuscript. Thanks are also due to Mr. Steve Castor for the excellent petrographic descriptions.

INTRODUCTION

The Klondike Mining district lies approximately 12 miles south of Tonopah, Nevada, on the east side of U.S. Highway 395. The mining area overlaps the Nye-Esmeralda County Line.

The primary flight line transects the mining area at a bearing of N. 30°W., and is approximately 6 miles long (Fig. 1). The two radar lines lie approximately 6 miles north and south of the center of the area and are oriented east-west. Access to the site is provided by several dirt roads.

PREVIOUS WORK

Albers and Stewart (1965), mapped the geology of Esmeralda County in preliminary form at a scale of 1:200,000. The geology to the east in Nye County, was mapped in preliminary form by Henry R. Cornwall in 1967. Albers and Stewart will publish a report on the geology of Esmeralda County in the near future. A few articles and abstracts have been published by Albers or Stewart dealing with the stratigraphy and structural geology.

E. R. Chipp (1969) in an unpublished M.S. thesis from the University of Nevada prepared a detailed study of the geology in the Klondike

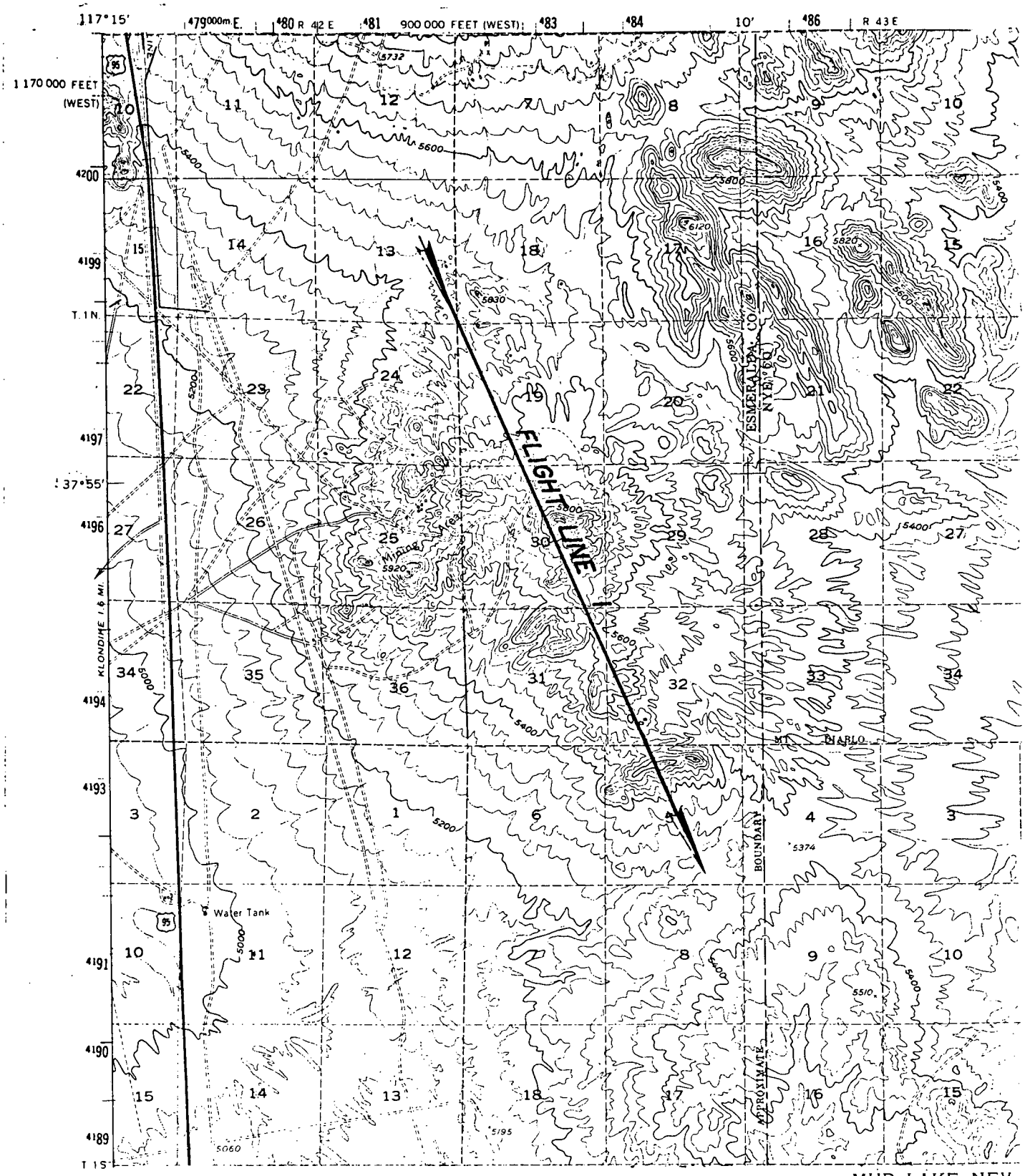

INDEX MAP OF THE KLONDIKE MINING DISTRICT

Figure 1.

area which includes a more complete definition of the mechanics of ore deposits. Approximately 10 square miles were mapped at a scale of 1:13,644 and 1/10 square mile at 1:2,400 scale. Emphasis was placed on the stratigraphy, structures, and alteration.

HISTORY

The silver deposits in the Klondike area were discovered in March, 1899, by J. G. Court and T. J. Bell. Vanderburg (1936, p. 79) reports that Chinese placer miners were working the area in the middle 1870's.

Most of the mining activity was in the years prior to 1905, from 1908 to 1910, and 1912 to 1925. After 1925, a few sporadic revivals accounted for minor production. The latest publically disclosed production was in 1959, which may have come from the area designated as the Klondike Peak mining area. The original claims by Court and Bell in the southern part of the main mining area, were the most productive.

PRODUCTION

The mines in the Klondike area produced chiefly silver with minor gold, lead, and copper. The recorded production is:*

*after Hewett, et. al., 1936, p. 59.

1903-1932.....	16,606 tons of ore yielding,
	2,405.64 oz. gold
	425,583 oz. silver
	10,861 lbs. copper
	257,080 lbs. lead
	value in all.....$529,052
prior to 1903.....	less than.....$ 25,000
	total.....$554,052 approx.

PALEOZOIC STRATIGRAPHY

CAMBRIAN SYSTEM

Cambrian age rocks are the most abundant and important hosts for ore deposits in the Klondike Hills. The Lower through Upper Cambrian is represented by three formations, which have been subdivided into a number of mapped units. This conformable sequence is limestone with interbedded siltstone and shale.

The Cambrian sequence has been metasomatized to a varying degree and locally indurated and changed to hornfels by contact metamorphism. In the northern part of the Klondike Hills, a representative exposure dips steeply to the east on the north limb of a syncline.

Harkless(?) Formation (Ch)

Only the upper most unit of the Harkless (Ch) appears on the geologic map. It is a bleached and recrystallized limestone and is massive to thickly bedded. The Harkless appears in the mapped area as a very thick sequence of alternating blue gray and tan crystalline limestone. The unit weathers into a friable calcitic sand where coarsely crystalline and the relatively unaltered beds stand only slightly above the other subdued areas.

Mule Spring Limestone (Gm_s)

The Mule Spring Limestone of Stewart and Albers is a massive to thickly bedded, blue gray limestone about 400 feet thick in the Klondike area.

Bold outcrops, algal forms, and a lack of chert and silicification in Mule Spring Limestone make it an excellent marker bed. Bedding varies from a few inches to more than 10 feet. It is finely crystalline except where coarsened by recrystallization near granitic intrusives.

Emigrant Formation

The Emigrant Formation makes up approximately half of the outcrops in the Klondike area. The basal argillite has acted as host for most of the granitic intrusive rocks, and as a lubricant for movement between the two lowest units. It has apparently been thickened and thinned tectonically. The permeability of the argillaceous limestone unit (Ge_2) has allowed this unit to be easily altered and the carbonaceous content has acted as a possible reducing agent for ore solutions. The overlying unit (Ge_3) is a spotted and indurated, relatively impermeable siltstone. The Ge_4 unit of the Emigrant Formation is a monotonous series of flaggy limestone with chert interbeds. The Ge_5 unit contains shale interbedded with the thin-bedded limestone and is characteristically banded.

Argillite unit (Ge_1). The basal unit of the Emigrant Formation in the Klondike area is a tan to white argillite averaging more than 50 feet thick. In the southern part of the area, this unit has been locally silicified or spotted forming a low-grade hornfels. The argillite forms outcrops with low relief and the rock commonly weathers light brown or lilac gray.

Argillaceous limestone unit (Ge_2). The Ge_2 unit is dominantly a dark gray, thin-bedded, locally silicified argillaceous limestone.

In the northern area the Ge_2 unit is 200-400 feet thick; bedding plane movements with local thrusting over the lower argillite unit suggest that the unit is thickened and thinned tectonically. The unit is partially silicified. In the northern area, the Ge_2 unit forms resistant ridges with angular fragments of silicified limestone and chert on the surface. Where silicification is less intense, outcrops erode to low forms.

In the southern area the Ge_2 unit has been extensively disected and brecciated by faulting and folding. There, a very fine-grained black weathering wholly recrystallized quartzite upholds ridges and forms bold scarps. This dense resistant unit approximately 20 feet thick dominates the remaining hundred feet or more of the easily weathered pelitic section. Along the northwesterly extension of the

Ge_2 exposures in the south area, the resistant quartzite is absent, presumably due to tectonic thinning.

The quartzite has a high density (2.63 gms/cc), relative purity, low porosity (approx. 4%) and microscopic texture consisting of a mosaic of interlocking grains averaging about .05 mm in diameter which give the unit a very high thermal diffusivity, making it an infrared marker horizon. The fine-grained matrix of this rock is cross cut by veinlets having larger grain dimensions, averaging about .20 mm. Iron hydroxide occurs as irregular masses in the rock and in the veinlets. A few irregular clots of hydromuscovite are present. Apatite occurs as irregular granular clots, as separate euhedral to subhedral crystals and in the veinlets in association with iron hydroxide. An acicular mineral in association with the apatite is probably dahlite and finely divided nearly opaque clots are probably collophane. This wholly recrystallized rock is probably the result of hydrothermal alteration of a phosphate cemented quartz arenite.

Spotted siltstone unit (Ge_3). The spotted siltstone occurs only in the northern part of the area. It thins rapidly to the northeast, but is estimated to be more than 100 feet thick southwest of Klondike Peak. It is usually dark olive brown with black or gray ovoid spots

up to 5 mm long. The siltstone has been partially silicified and converted to a low-grade hornfels by contact metamorphism. The unit weathers to low hills composed of angular blocks and flat chips (Fig. 2).

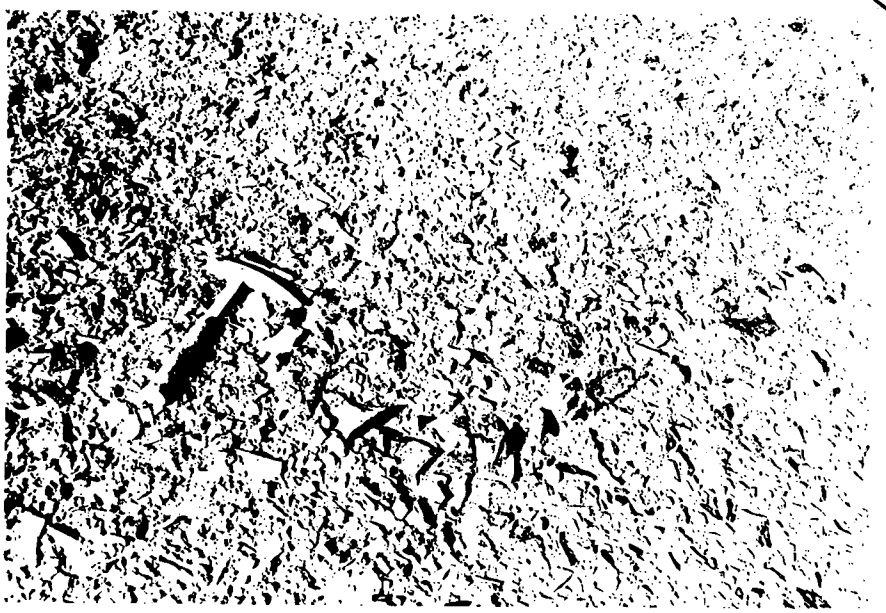

Figure 2. Weathering surface of the Spotted Siltstone (Ge_3).

Limestone unit (Ge_4). The limestone unit of the Emigrant Formation is the most extensive and probably exceeds 2000 feet in thickness. In the northern area it is conformable over the spotted siltstone, but to the south its northern edge has been thrust over the uppermost unit of the Emigrant Formation.

The limestone is dark blue-gray and flaggy with chert interbeds not exceeding 3 inches, but commonly less than 1 inch. Chert beds

occur almost rhythmically every 5 inches or less. East of the main mining area, zones up to 100 feet wide are silicified and bleached white. The limestone weathers to moderate forms except where it is highly siliceous.

Banded unit (Ge_5). The banded limestone and shale unit is readily discernable on the weathered surfaces by thin alternating red, brown, and gray colored bedding bands less than 1/2 inch thick. Within the erosional window to the south between the two thrust plates, the banded unit contains dark gray shale beds up to 10 feet wide. The more shaly facies may have been faulted out in the northern area.

The banded unit in the north is locally bleached and silicified with areas of hornfels mineralization. The sequence to the south is not as altered and weathers to forms with low relief (Fig. 3). The unit is 500 feet thick in the northern area and estimated to be approximately 700 feet thick to the south.

ORDOVICIAN SYSTEM

Palmetto Formation

The Ordovician Palmetto Formation consists of approximately one thousand feet of black and grey eugeosynclinal sediments. For the

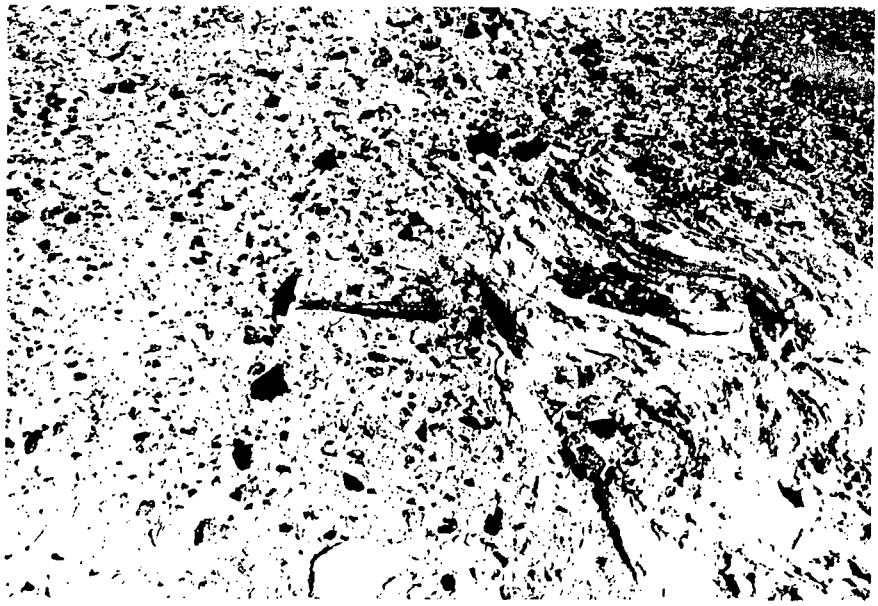

Figure 3. Outcrop and weathering surface of the banded unit (Ge_5) of the Emigrant Formation.

purposes of this study the Palmetto has been subdivided into six stratigraphic and two non-stratigraphic units.

Shale unit (Ops). The lowermost exposed unit of the Palmetto consists mostly of medium gray shale that weathers to a "woody" appearance with a slight lavender tint. The shales are interbedded with thin bedded dark gray graptolitic limestones. Near the top of the shale is a distinct tan weathering tremolitized bed. The unit weathers to densly packed angular fragments (Fig. 4).

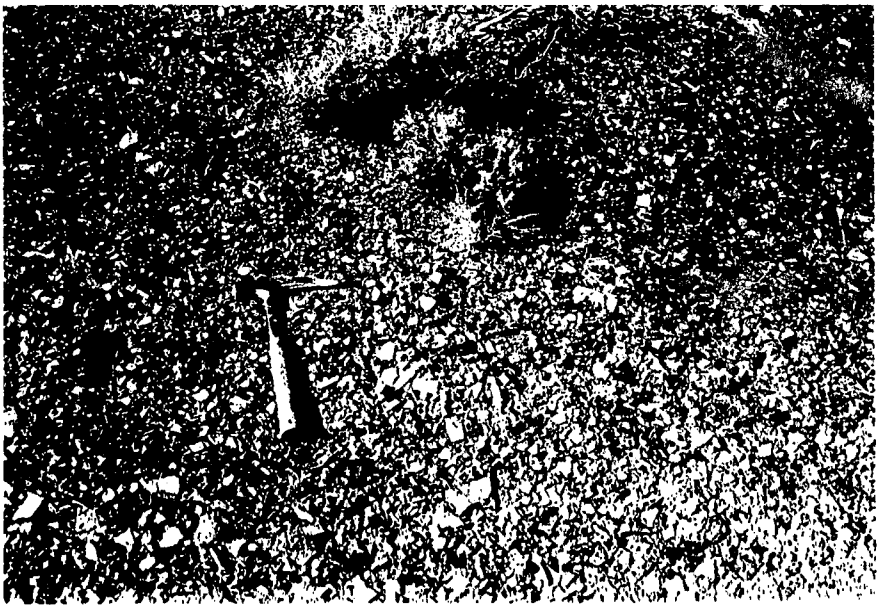

Figure 4. The shale member of the Palmetto Formation weathers to angular pebble size fragments with dense packing.

Limestone unit (Opl). The Opl is a massive resistant medium gray limestone. Laterally this unit may grade into a rhythmically stripped limestone and chert or chert sequence.

Chert unit (Opc). This black chert unit grades laterally into a gray cherty limestone and it is probably the top of the Opl unit. It is separately mapped because of its distinct color and thermal properties.

Tremolitized unit (Opt). The Opt unit is a series of gray shales,

limestones and tremolitized sediments. This unit is not subdivided because it is normally covered by talus from the overlying ridgeforming quartzite.

Quartzite unit (Opq). This gray to black to tan to white quartzite is the dominant ridgeforming unit in the Palmetto. It may occur as one massive quartzite ledge 30 or more feet thick or as up to a half dozen thin quartzite beds interbedded with soft light gray shales. The quartzite weathers to large irregular blocks stained dark brown to dark gray (Fig. 5).

Figure 5. Quartzite member of the Palmetto Formation.

Upper limestone unit (Opls). The uppermost exposed beds of the Palmetto consist of several hundred feet of medium gray limestones interbedded with black chert. The chert and limestone bands several inches to a foot wide make the unit very distinctive.

Dolomite unit (Opd). The Opd is a discontinuous map unit. It consists of a tan to cream hydrothermal sanded dolomite. Opd is known to occur at the Opl, Opt, and Opls horizons and except for coloration weathers identically to these units (Fig. 6).

Figure 6. Dolomitic limestone (Opd) member of the Palmetto Formation weathers to light brown semiangular fragments.

Secondary chert unit (Opc). The discontinuous Opc is lithologically identical to the stratigraphic Opc unit. This black chert is developed along the contact with many rhyolitic intrusions, fault contacts and mineralized zones (Fig. 7).

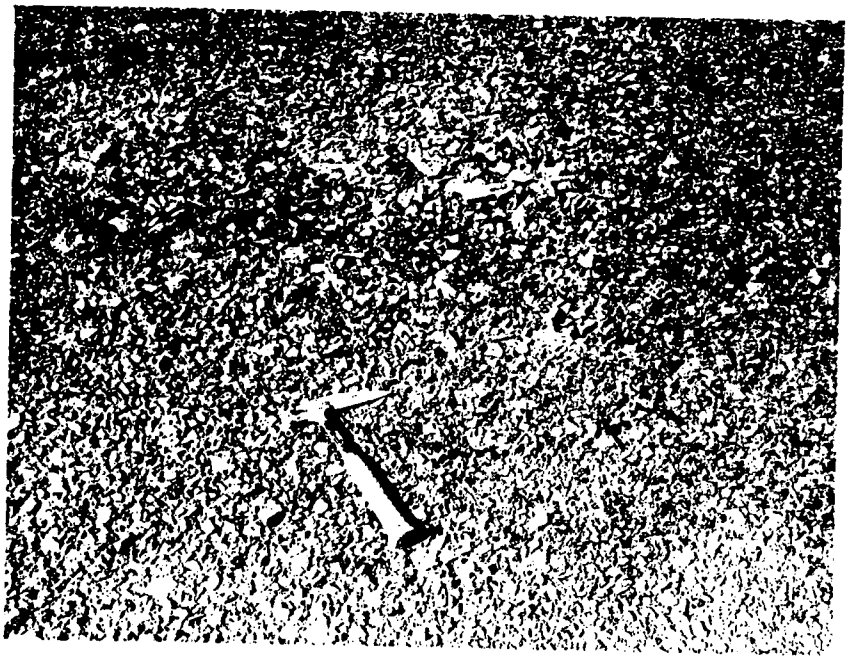

Figure 7. Black chert (Opc unit).

IGNEOUS AND VOLCANIC ROCKS

TERTIARY SYSTEM

Granite

The granitic rock occurs as two small irregular knobs with short discontinuous sills between, as well as a few other sills to the north. The granite outcrops in a trend N.60°E. A few fine-grained granitic dikes intrude the adjacent units at right angles or obliquely to the N.60°E. trend.

The granite is a leucocratic, medium-grained muscovite granite with local fine-grained border facies and small quartz-muscovite pegmatitic facies. The granite weathers black (Fig. 8), apparently from manganese and iron released by supergene processes.

Ash flow tuff (Taf)

A rhyodacite ash flow tuff (Taf) is distributed around the borders of the Klondike Hills. It lies unconformably upon the lower Paleozoic sediments and is commonly covered by the rhyolite flows.

The ash flow tuff contains more than 50% crystal and pumice fragments and exhibits moderate welding. Feldspar crystals are mostly subhedral grains and are partly replaced by calcite, sericite and clay

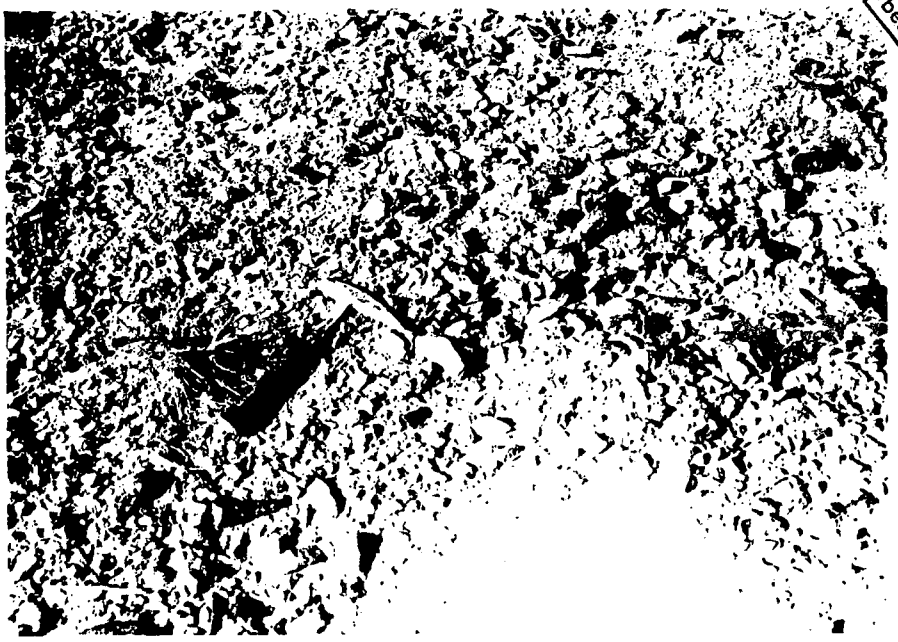

Figure 8. The muscovite granite; note the black manganese coating on many of the fragments.

(montmorillonite?). The original biotite grains are replaced by sericite with a little chlorite and iron oxide.

The larger glass shards show spherulite structure and alignment of the shards and crystals produce a distinct directed texture.

The unit characteristically weathers into low mounds and contrasts with the rhyolite units by its persistant pale olive green color.

Andesite (Ta)

The andesite occurs in small patches bordering the Klondike Hills. It apparently has intruded(?) the older rhyolites and ash flow tuffs,

however, the vesicular structure it exhibits is more indicative of a flow rock or very near surface intrusion.

Most of the andesite is porphyritic in nature and is comprised of plagioclase and altered mafic phenocrysts in a light brown microcrystalline matrix. The plagioclase phenocrysts are mostly euhedral or subhedral with an average composition of An_{40} to An_{45}. The plagioclase is partially altered to calcite and clay with minor amounts of sericite present. Yellow green chlorite occurs in the rock as alteration of the hornblende and biotite crystals. The calcite and chlorite show circular shapes and probably filled vesicles within the rock.

In the northeastern portion of the flight line the andesite has been extensively propylitized and highly oxidized. The original hornblende and pyroxene grains have been entirely replaced by septechlorite and chlorite. The andesites in this area have undergone propylitic alteration followed by a period of strong oxidation.

Most andesite contacts in the Klondike area are obscured by alluvium, as the andesite weathers rapidly to very subdued mounds (Fig. 9). The andesites are probably of several age periods, some prior to the rhyolite intrusion and flows, and some appear to have intruded the rhyolite units.

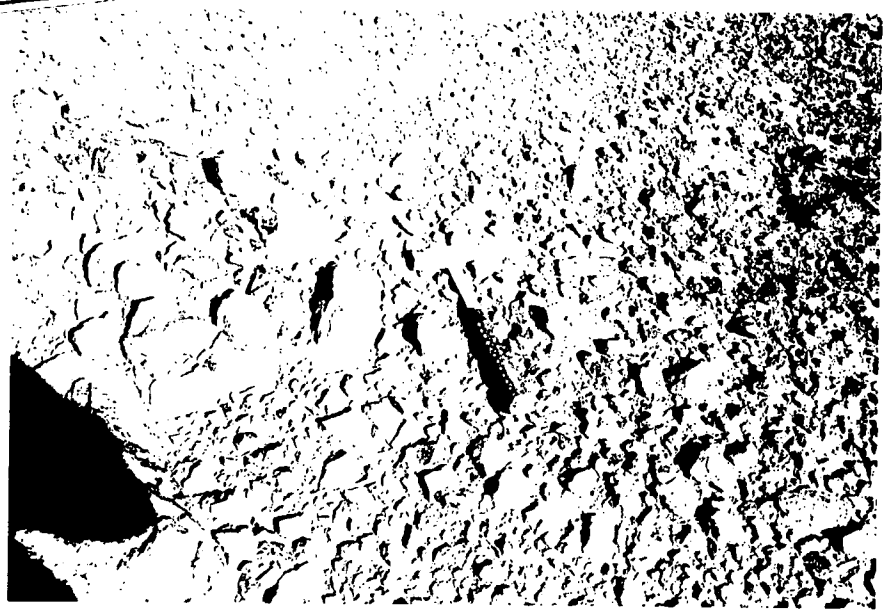

Figure 9. Surface of andesite flow.

Rhyolite (Tr, Tri, Trs)

The rhyolite units occur throughout the Klondike area as flows, dikes and eroded plugs. The extrusive units transgress into intrusive contacts without appreciable change in texture and/or composition. The unit appears as volcanic domes, flows, flow breccias and tuffs, in the border areas of the site and as dikes where erosion has exposed the Paleozoic units. Many dikes outcrop for long distances and occupy fault dilations. The highly silicified portions of the rhyolite unit

(Trs) form the prominent knobs in the northern portion of the area but the rhyolite generally weathers to subdued mounds except in the case of plugs (Fig. 10).

Figure 10. Weathered surface of rhyolite dike.

The ash flows included in the rhyolite unit are approximately half devitrified glass shards with volcanic dust and half crystals by volume. Quartz crystals as large as 3 mm are common and are partly rounded. Secondary(?) quartz has flooded the matrix and in the case of the Trs unit secondary quartz and illite constitute 80% of the volume.

Most of the rhyolites exhibit hydrothermal alteration, with the

biotite being replaced by sericite and clay. In some samples the glass shards have a welded appearance and the larger shards are moderately aligned. Small breccia pipes occur around the intrusives and these areas display intensive hydrothermal alteration.

Fraction(?) Breccia (Tf)

In the mapped area the Fraction(?) Breccia of the Siebert Formation of the Divide district is a welded crystal-lithic quartz latite or rhyodacite tuff. The unit generally underlies the uppermost members of the rhyolite unit and lies on top of the older rhyolite flows.

It is a crystal lithic tuff consisting of 30-35% crystals and 10% lithic fragments in a matrix made up of glass shards and volcanic dust. Locally the biotite is badly corroded with some alteration to muscovite, chlorite and iron oxides. A very poorly defined flow structure is present and some shards show a swirled texture with moderate amounts of welding.

In the mapped area the Fraction Breccia is slightly more resistant to weathering and forms more outcrops than the rhyolite. Where the Fraction has not been intensely altered, its surface coloration is tan to light brown. Locally it may be bleached and is identifiable only by texture from the rhyolite units.

Basalt (Tb)

Thin flows of basalt cap isolated hills to the extreme east. These flows probably do not exceed 50 feet in thickness and overlie intrusive rhyolites. The composition of the basalt varies from fine-grained, holocrystalline, olivine basalt to hypersthene basalt with trachytic texture.

ALLUVIAL AND LACUSTRINE DEPOSITS

QUATERNARY SYSTEM

Tufa

A calcareous tufa of probable hot spring origin occurs in a limited area to the extreme south. It is a tan, amorphous, calcareous rock with small dark specks and a few brown aragonite nodules. It unconformably overlies small patches of the ash flow tuff, and the rhyolite. It is not tilted and contains no incorporated detrital material. An age of post-rhyolite and pre-Recent alluvium is tentatively assigned to the deposit.

Alluvium

Poorly integrated large drainage networks radiate away from the Klondike Hills. Fluvial sand and gravel with large angular boulders fill subdued areas in the hills and along the periphery. Colluvium at the base of the steeper slopes contain abundant angular blocks and the numerous gullies are alluviated with sand and gravel.

STRUCTURE

The macro structure of the Klondike Hills is a faulted and folded syncline, 2 miles wide and 4 miles long. The fold axis trends approximately N.60°E. and plunges to the northeast. The syncline is complicated by local anticlinal folding with the same approximate trend, and anticlinal folding with imbricate thrusting along the southern limb. Right-lateral strike-slip faulting has produced minor flexures, and controlled the emplacement of the rhyolite dikes. North trending, late Tertiary Basin and Range normal faults in the eastern portion of the area are downdropped on the east side.

THRUST FAULT INVOLVING THE PALMETTO FORMATION

The Palmetto thrust involves only the Palmetto Formation and the uppermost Emigrant unit. The thrust may have eliminated the uppermost few hundred feet of the Emigrant Formation.

THE HICKS FAULT

The Hicks Fault strikes approximately E-W, dips steeply, and separates the main mining area into two segments. The vertical displacement is near 1500 feet with the north side downdropped.

SYNCLINAL FOLDING AND BEDDING PLANE FAULTS

The syncline was folded along an approximate N.60°E. axis. The trough of the syncline is anticlinally folded along with other smaller folds.

The thrusting between the Ge_2 and Ge_1 units in the north is most clearly seen to the extreme northwest where the Ge_2 unit has locally overthrust the Mule Spring Limestone. The local thrusting in the northwestern area was probably due to differential movement during the synclinal folding.

SOUTHERN THRUSTS AND RELATED FAULTING

The Ge_2 unit to the south has been imbricated by thrusting with considerable brecciation and silicification. Locally, brecciated fault zones occur en echelon within the Ge_2 unit. The Ge_2 unit is thrust over the Harkless(?) Limestone and the Mule Spring Limestone along the western part of the anticlinal exposure.

The limestone unit (Ge_4) of the Emigrant Formation is thrust north over the uppermost unit (Ge_5) of the Emigrant Formation just south of the Palmetto thrust plate and north of the thrusting in the south.

Numerous small and large faults trending approximately N.40°W.

appear to be part of a conjugate shear system from compression along a N-S axis. Some may be tear faults related to the thrusting in the south. The down-side is usually to the SW and they are probably right-lateral strike-slip with minor vertical offset. The major fault north of Klondike Peak has 1500 feet of relative right-lateral movement and the units on either wall are broadly warped.

Rhyolite dikes occupy the NW breaks and the three prominant peaks have their long axis northwest. Short but relatively wide dikes occur near some N.40°W. trending dikes, with trends near E-W or N-S. A rhyolite dike parallels the anticlinal axis in the southern area, apparently occupying a tensional break that occurred during folding.

BASIN AND RANGE NORMAL FAULTS

Late Tertiary normal faults typical of the Basin and Range trend near N-S in the eastern part of the Klondike area. Scarps are still visible along the east side where north-trending faults have down-dropped the east side.

ORE DEPOSITS

In all areas mined, quartz veins less than 10 feet wide, and commonly 1 to 2 feet wide, occur parallel or subparallel to bedding. The quartz veins are locally brecciated and commonly pinch out laterally or vertically within a few tens of feet. In the main mining area, the veins dip approximately 30° to the east and occur within local zones of movement or dilation in the Ge_2 unit. Quartz veins in the eastern Klondike mining area dip 45° east, and occur within the Palmetto thrust zone or a few feet above the thrust contact in argillaceous limestone beds of the Palmetto Formation. In the Klondike Peak mining area, the quartz veins are thinner with slight dip to the southeast.

HYPOGENE MINERALIZATION

Galena, pyrite, and bornite are the only identifiable primary sulfides. Galena and pyrite are the most abundant and constitute less than 5% of the vein material where oxidation was not complete. These minerals are found as small isolated crystals or rarely in small clusters within the quartz gangue. The less shattered vein quartz protects the sulfides from oxidation. In all cases, however, galena is found with borders of cerrusite and minor anglesite, which may have

protected the galena from further oxidation. Workings are shallow and samples deeper than approximately 100 feet were unobtainable. Scheelite occurs in one thin vein in the main mining area while other mineralization is lacking. A yellow garnet similar to that found in the jasperoids within the Mule Spring Limestone, occurs in the quartz veins to the extreme northwest of the main mining area. Except for the sericite seen in thin-section, milky white quartz is the main gangue material.

Bornite is rarely found as small islands (less than 0.1 mm) within a mixture of digenite and covellite. Digenite (Cu_9S_5) replaces bornite and in turn is replaced by covellite.

The galena and other minerals apparently do not contain any exsolved minerals. The silver minerals are unknown. Galena may be argentiferous, or silver minerals may be associated with the bornite and digenite. Assays of the relatively unoxidized samples indicate less than 10 oz. silver per ton. The thoroughly oxidized vein material with abundant cerrusite, jarosite, and iron oxides, assayed from 90 to 210 oz. silver, and 0.13 oz. gold per ton. Spectrographic analysis of the sulfide material seemingly eliminated the possibility of antimony or bismuth minerals.

OXIDATION AND SUPERGENE MINERALIZATION

The less oxidized samples contain galena replaced in part by cerrusite, with minor covellite, malachite, and chrysocolla. Pyrite is usually replaced by hematite, which alters to limonite, and locally the pyrite is replaced by cerrusite. Bornite is replaced by digenite, which is probably of supergene origin along with the covellite. Covellite occurs along the crystal borders outside the inner zone of digenite, and malachite and chrysocolla occur beyond the crystal borders. A fine-grained sooty material between the covellite and malachite may be chalcocite. Galena is mostly altered to cerrusite, but locally, covellite replaces galena along cleavage planes or crystal borders. Cerrusite forms borders around the galena or replaces the galena along fractures. Malachite with chrysocolla locally form borders outside the cerrusite border. In all cases where malachite and chrysocolla occur, malachite forms next to the cerrusite with chrysocolla outside adjacent to the quartz. In one example, malachite in rosettes of prismatic crystals forms a base for the chrysocolla.

Most of the oxide ore that was mined is a mixture of cerrusite, jarosite, hematite, limonite, and possibly wad. Cerargyrite (AgCl) is reported to be the main silver mineral, but was not positively identified.

Jarosite apparently contains no lead or silver by specific gravity measurements (3.18). At depth, the early miners rejected the more dense vein material with sulfides for the thin-walled quartz boxworks filled with oxidation minerals.

Stetefeldite $(Ag_{1-2}Sb_{2-1})(O,OH,H_2O)$ was thought (Spurr, 1906, p.375) to occur sometimes in a black earthy material consisting of a mixture of chalcocite and pyrite. The black material mentioned by Spurr in the Klondike ore, was determined by X-ray diffraction to be cerrusite with minor anglesite. No peaks near those of stetefeldite were found. A yellow earthy material with occasional crystalline form was suspected to be the mineral, but had all the optical qualities of jarosite.

Jarosite occurs as massive material filling cavities formerly occupied by pyrite or galena, as well as the yellow earthy material associated with cerrusite and iron oxides. Fine-grained supergene quartz and calcite is observed in thin-section, later than the sulfides and contemporaneous with the cerrusite.

DISCUSSION OF ORE DEPOSITS

During the late Mesozoic(?), granitic intrusions at depth produced contact metamorphism and metasomatic alteration. Quartz veins formed in zones of brecciation and dilation, which are the tectonic zones

created by the Palmetto thrust of early Mississippian(?) age, and the bedding plane thrusts of late Mesozoic age which were produced during the synclinal folding. Contemporaneous with the formation of the major quartz veins and beyond the zone of pervasive silicification, the carbonate veins define an extended zone of mild alteration. A halo of pyrite formed closer to the ore deposits within the zone of silicification. The pyritization and silicification, however, are confined mostly to the hanging wall of the bedding plane thrusts (the Ge_2, Ge_3 and Ge_4 units). Pyrite is not abundant and commonly oxidized to jarosite, hematite, and limonite.

Within the zone of pyritization and close to the ore deposits, the muscovite granite shows a late stage of sericitization with minor silicification. Sericite is also associated with the ore minerals in the quartz veins, and the later quartz veins in the Ge_2 and Ge_3 units. Sericite is seen only in thin-section. Galena, pyrite, and bornite constitute the primary ore with pyrite probably forming first. Galena is rarely found enclosing cubes of partially replaced pyrite. It is not known whether this pyrite is from the earliest stage of alteration or an early formed pyrite in the ore forming stage.

Oxidation and supergene sulfide enrichment is an important consideration in further exploration of the district. Uplift and doming occurred

soon after the muscovite granite intrusion, and probably intermittently up to the present. The Hicks Fault may be the result of this doming. Ash flow tuff on both walls of the fault, and possibly on the muscovite granite, supports the fact that in early Miocene time the area had been eroded considerably and the granite was deroofed. Possibly any concealed ore deposits that at one time had been exposed to oxidation near the surface, may contain the halide silver deposits, or enriched copper and silver concentrations.

Mining in the Klondike area has been almost entirely within the halide silver deposits. Small shipments containing less silver but more lead and copper are reported intermittently during the later years of production. The slightly enriched material was probably stockpiled, concentrated and shipped at an opportune time.

AIRCRAFT FLIGHT SUMMARY

During August of 1970 NASA Mission 140 was flown over the Klondike District, Nevada. The geologic test site in the Klondike area was chosen for a number of reasons. The area provided a site with year-round accessibility, low relief, minimum vegetation, and good rock outcrops. Additionally, it was found to have little or no microwave interference and had already been mapped by E. R. Chipp.

The NASA 927, P3A Electra II aircraft was used for the mission. This four engine aircraft provided a stable platform for the two metric cameras, multispectral camera cluster, thermal infrared scanner, multi-frequency microwave, side looking airborne radar (SLAR), and PRT-5 infrared radiometers used on this experiment.

Tables 1, 2 and 3 review the flight parameters, instrument systems parameters and photographic parameters for Mission 140. Individual instrument specifications are discussed in the following sections along with the data obtained from each instrument system.

Table 1. Mission 140 Flight Parameters - Klondike Mining District, Nevada.

Line	Run	Time Start	Time Stop	Altitude Baro in m	Altitude Radar in m	Heading	Pitch	Roll	Drift	Ground Speed Kts
Flight 9	8-15-70									
2	1	182450	182700	5200m	3400m	091	0	0	2.5°L	290
3	1	183220	183530	5200m	3500m	273	0	0	0	280
1	1	191920	192155	3000m	1100m	152	0	0	.0	152
1	2	192740	192955	3000m	1100m	151	0	0	.5°L	151
1	3	202410	202615	3000m	1200m	150	0	0	1 °R	150
1	4	203200	203420	3000m	1200m	150	0	0	2 °R	150
Flight 10	8-16-70									
1	1	103700	103845	3000m	1000m	180	0	0	1 °L	156
1	2	105130	105400	3000m	1000m	180	0	0	2.5°L	153
1	3	110100	110315	3000m	1000m	180	0	0	3 °L	154

Table 2. Mission 140 Instrument Operation - Klondike Mining District, Nevada.

Line	Run	Cameras RC 8	Cameras KA62	Infrared 8-14μm RS-14	Infrared 8-14μm PRT-5	Microwave Polar	Microwave Elev.	Microwave Boresite	Radar SLAR
Flight 9	8-15-70								
2	1				X				X
3	1				X				X
1	1	X	X	X	X	V	0°	X	
1	2	X	X	X	X	H	0°	X	
1	3	X	X	X	X	H	0°	X	
1	4		X	X	X	V	0°	X	
Flight 10	8-16-70								
1	1			X	X	V	0°		
1	2			X	X	H	0°		
1	3			X	X	V	0°		

Table 3. Mission 140 Photographic Parameters - Klondike Mining District, Nevada.

Camera Type	RC-8	RC-8	KA62	KA62	KA62	KA62
Format	22.9cm	22.9cm	11.4cm	11.4cm	11.4cm	11.4cm
Film	SO397	2443	SO246	2402	2402	SO117
Filter	HF3	15(?)	87B	29	58	15+CC30R
Shutter Speed	1/250	1/300	1/60	1/125	1/125	1/90
f Stop	5.6	6.2	4.5	4.5	4.5	4.5
Overlap	60%	60%	60%	60%	60%	60%
Intervalometer	5.5 sec	5.5 sec	-	-	-	-

COLOR PHOTOGRAPHY

PHOTOGRAPHIC EQUIPMENT AND PARAMETERS

Color and color infrared photography were obtained using two Wild RC-8 metric cameras and one camera from the KA62 multispectral cluster. The RC-8 aerial survey cameras employ a 22.9cm x 22.9cm format and use a 15.2cm focal length, f 5.6 Aviogon lens. The cameras are designed with a vacuum platten and rotary shutter with continuously variable shutter speeds of from 1/100 to 1/400 of a second. They are designed for a maximum cycling speed of 3.5 seconds and carry a 225 frame magazine.

For the Klondike site a flight altitude of 1000 meters was chosen. A 5.5 second intervelometer setting at this altitude yielded photography with an initial scale of 1:6000, 60% overlap and a ground resolution of approximately 18 cm in medium contrast terrain. The multispectral cameras yield as initial scale of 1:12,000 from this altitude and have an approximate ground resolution of 30 cm. The metric photography shown in this section have been reduced by 50% to conform to the 1:12,000 scale of the multispectral photography and the geologic mapping.

One metric camera was loaded with Aero Ektachrome film type S0397 with a haze filter which serves to exclude ultraviolet and a portion of the violet where maximum haze scattering occurs. Excellent photography both from the standpoint of resolution and color quality was obtained from this camera.

The second metric camera was loaded with Aero Infrared Ektachrome type 2443 film and fitted with a Wratten #15 (minus blue) filter (see

Figure 11). Either because of film age, overheating, manufacturing error or processing the resulting transparencies had virtually no infrared sensitivity. The processed film was entirely unusable shades of blue and green. The result forced heavy reliance on the Ektachrome photography.

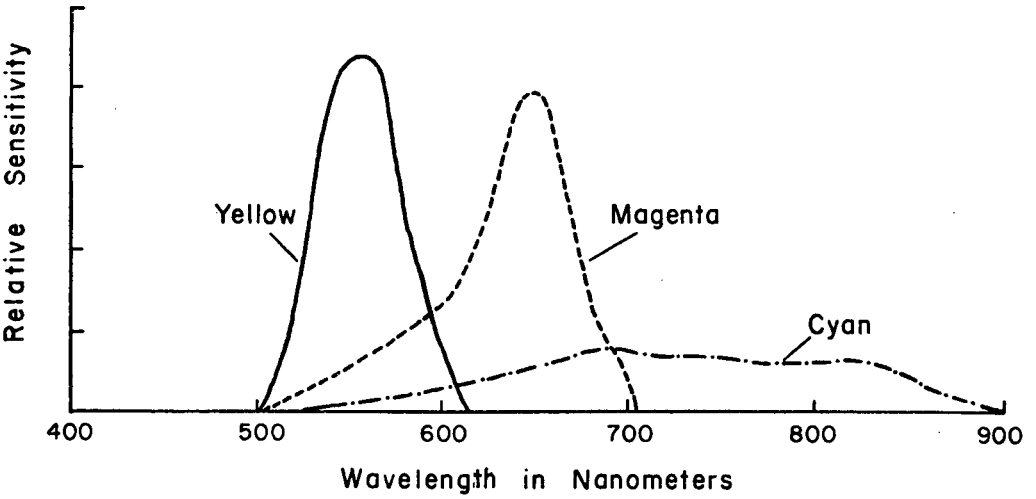

Figure II Ektachrome type 2443 infrared film (color), Wratten No. 15 Filter.

One camera of the KA-62 cluster (described in the multispectral section) was also loaded with Aero Infrared Ektachrome type SO117 and Wratten #15 and #CC30R filters (see Figure 12). Because color IR films are primarily designed for vegetation analysis and vegetation is ultra-reflective in the near infrared the film is manufactured with a relatively less sensitive infrared layer (Figure 11). Geologic targets are not ultra-reflective in the infrared so in order to bring up the relative sensitivity of the infrared layer a #CC30R filter was used in conjunction with the normal minus blue filter (see Figure 12). This configuration should have resulted in the portrail of relatively more near infrared geological

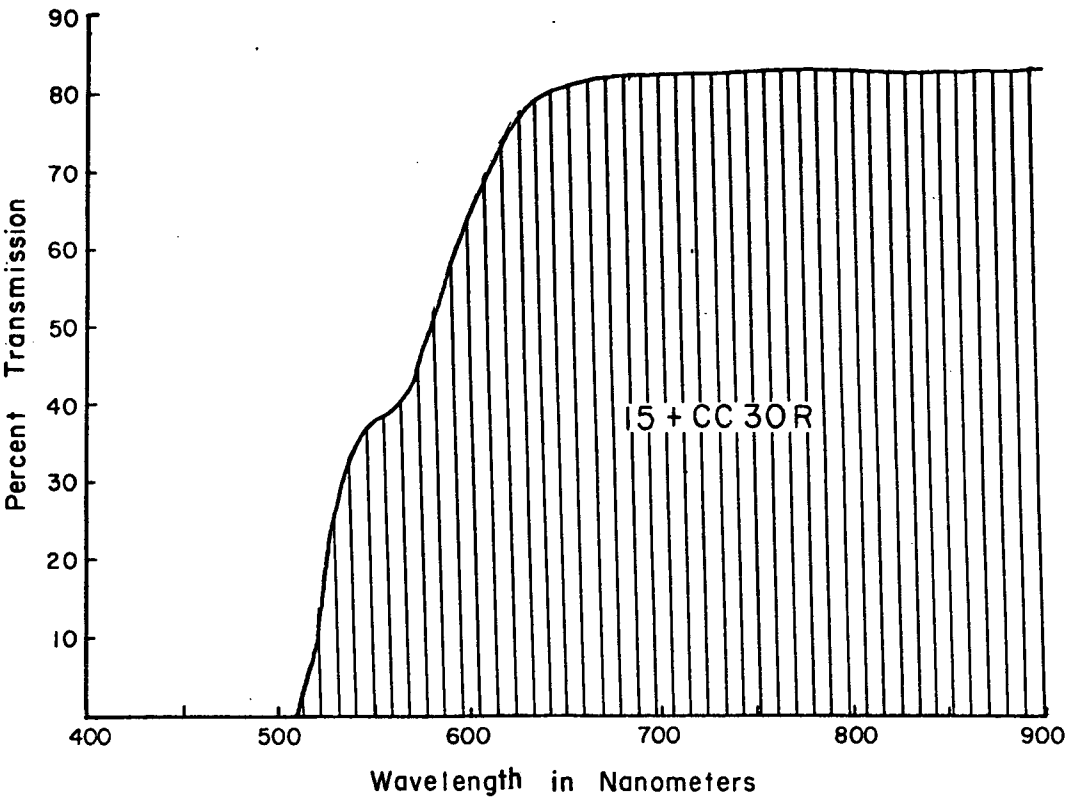

Figure 12 Transmission of Wratten No. 15 plus No. CC 30R Filters

information and the elimination of the usual blue or green tint to the photographs. Healthy vegetation photographed with this filter combination should be highly overexposed in contrast to geologic targets, and is probably of little use in botanical studies. Unfortunately the infrared film in this camera like that in the second metric camera had defective infrared sensitivity. The infrared sensitivity of this film was only a fraction of that normally obtained on some targets with very high infrared reflectivity and the data was deemed unworthy of detailed analysis.

COLOR PHOTOGRAPHIC INTERPRETATION

Figure 13 shows a print of Ektachrome metric photography reduced to a scale of approximately 1:12,000. The area shown includes a portion of the northern volcanic field and the eastern portion of the main mining area along the Hick's Fault. Virtually all of the mappable units in the area may be seen on this photograph. The matching geologic map, Figure 14, shows the outcrop pattern of the various units and allows the determination of the range of colors exhibited by each of the various rock units. It should be noted that certain of the mappable rock units exhibit an extremely wide range of coloration. This is primarily due to alteration and bleaching along the Hick's Fault. Some of the rock units such as the Ta (andesite) are typified by local differential alteration and may be identified by their mottled appearance. Other units such as the Ge_4 are normally rather consistant in coloration. In the Hick's Fault area, however, the usually dark blue gray Ge_4 unit exhibits a white to tan bleached horizon as well as several zones with a lightened gray color. This peculiar coloration is not seen in the Ge_4 elsewhere on the test site. Other color anomalies occur on the photographs. The red-orange area in the Ge_4 near the center of the photograph is an oxidized hematite vein; several of the other small red-orange areas on the photograph represent locally mineralized areas and mine dumps resulting from excavations in the vicinity of mineralized veins.

Numerous faults may also be seen on the Ektachrome photography. They may be clearly seen either where beds are cut so as to have different topographic expressions on each side of the fault or where beds with

Figure 13. Ektachrome areal photograph of the northern volcanic area.

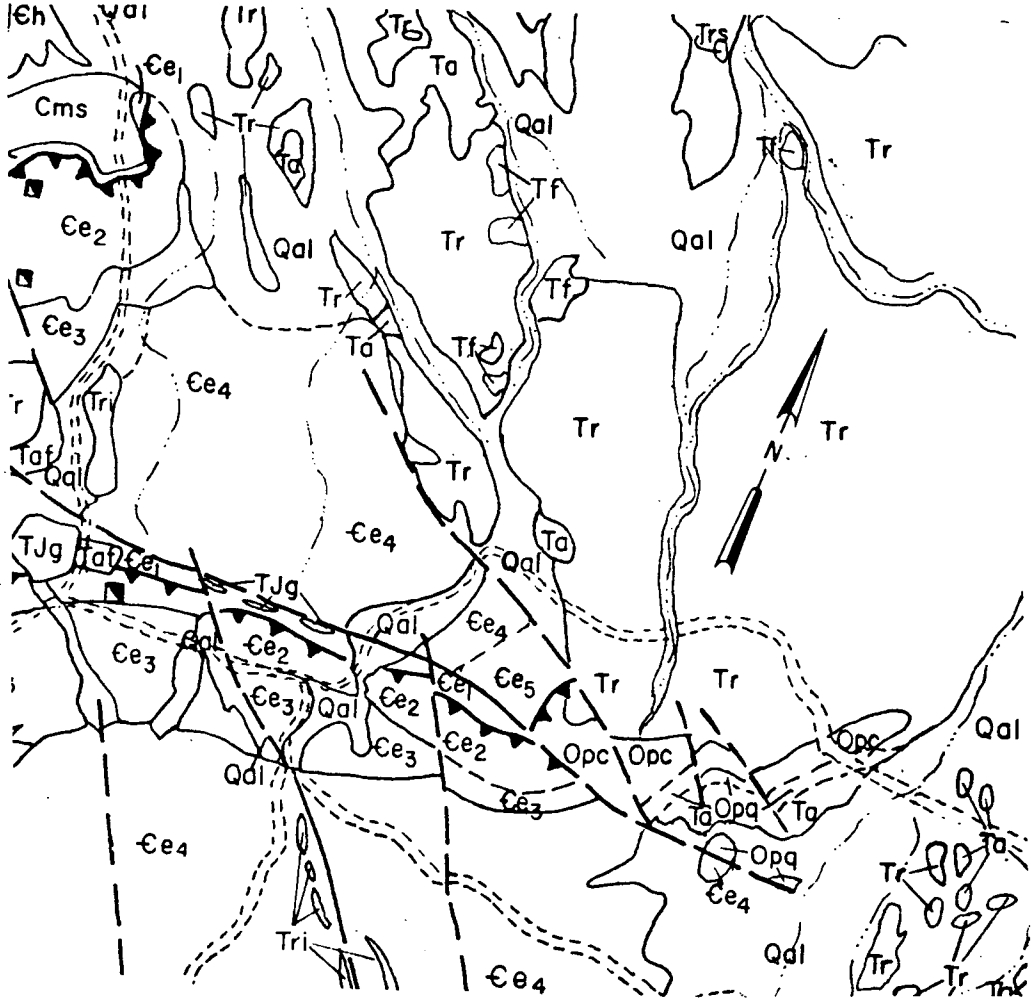

Figure 14. Geologic map for the northern volcanic area.

different coloration are offset against one another. Figure 15 shows a geologic map of the area along the Hick's Fault corrected from the color photography.

Figure 16 is an Ektachrome photograph of an area somewhat to the south of the area shown in Figures 13, 14 and 15. The sedimentary rock units exposed in this photograph are higher in the section than those in Figure 13. It is primarily Palmetto Formation (Ordovician). The same general comments about distinctive tones for the various rock units made for Figure 11 may also be made for Figure 16.

The three most prominently displayed geologic units on this photograph are Ordovician Palmetto Formation, Tertiary intrusive rhyolite and Quaternary alluvium. The alluvium exhibits its usual heterogeniety and the intrusive rhyolite is remarkably uniform. The Palmetto, however, shows a remarkable diveristy of coloration compared to the number of mappable stratigraphic units actually present. The Palmetto is a characteristically dark gray to black eugeosynclinal sequence composed of limestones, cherts, quartzties and argillites. In the lower left corner of the photograph almost the entire Palmetto sequence may be seen in an undisturbed and only slightly altered sequence. Along the bottom edge of the photograph about 2 cm from the lower left corner the base of the sequence may be seen. Proceeding upward on the photograph some 3 cm all but the top beds of the Palmetto may be seen.

Using this uninterrupted sequence as a guide to coloration, the rocks in the upper left corner of the photograph may be interpreted as dark cherts lying near the base of the sequence and the rocks to the

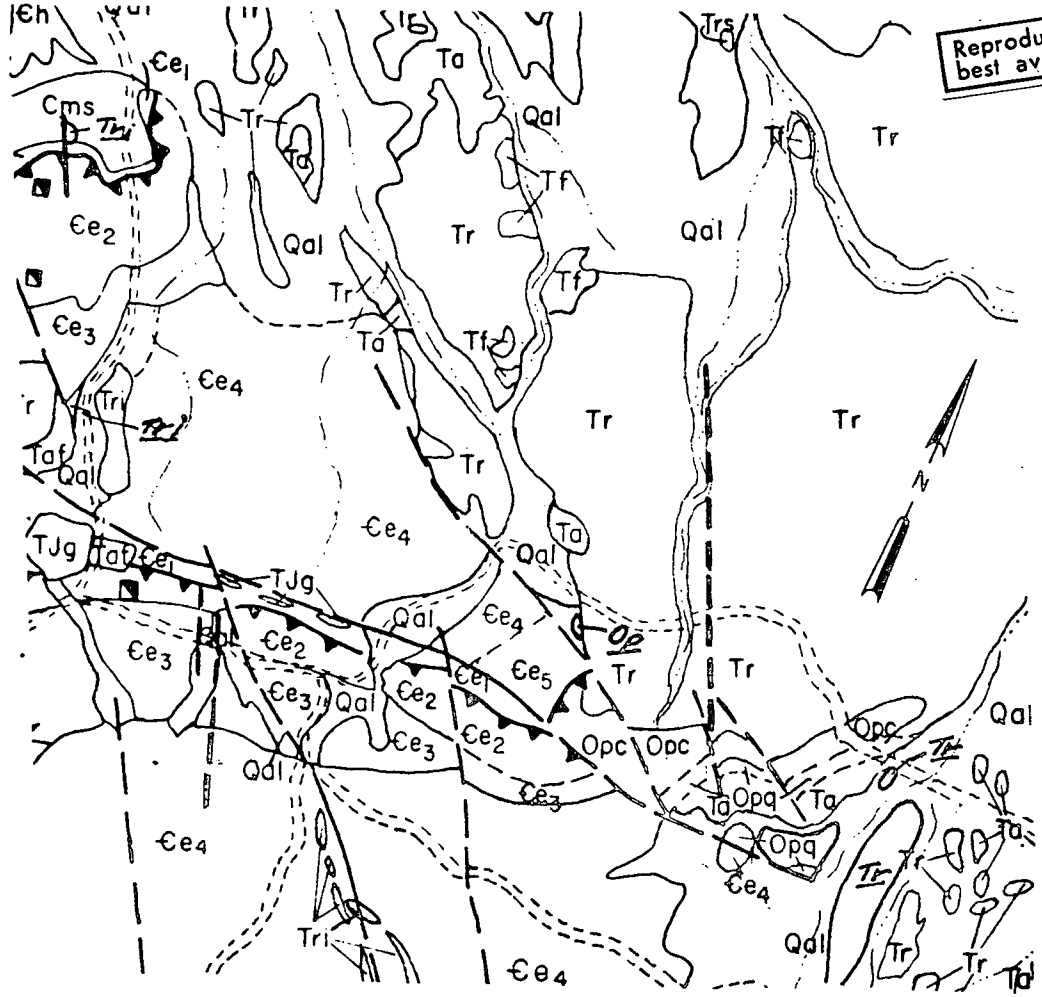

Figure 15. Corrected geologic map of the northern volcanic area along Hick's Fault.

Figure 16. Ektachrome areal photograph of the central portion of the test site.

right may be interpreted as the mottled center beds in the sequence. The medium gray units 2 cm below the top of the photograph and 3 to 6 cm from the right edge do not occur in the sequence described in the lower left of the photograph. They are light gray limestones with black chert partings which lie on top of the widely exposed Palmetto sequence.

Near the center line of the photograph 1.5 cm from the top, the black Palmetto chert fringing a rhyolite dike is an alteration phenomena. The chert is produced where silica-rich rhyolite solutions contact relatively porous limestone units. The orange or orange-brown coloration spotted throughout the photograph is also an alteration phenomenon and in each case the orange dolomitized areas occur in conjunction with rhyolitic dikes, faulting and the favorable middle units of the Palmetto Formation.

CONCLUSIONS

It is concluded from working with the color photography that it is quite superior to the black and white photography in altered terrain such as the Klondike Hills. Many of the features and geologic units have been identified because of their color rather than overall reflectivity (which is the parameter recorded by black and white photography). Color photography should be flown under clear skies and the solar intensity should be monitored during the flights to insure uniform exposures. A number of frames of color photography were ruined by spotty cloud cover during the three photographic runs over this site.

MULTISPECTRAL PHOTOGRAPHY

In recent years a new technique, multispectral photography, has entered the field of photographic target identification. This technique allows the investigator to select specific portions of the visible and near infrared spectra to produce maximum contrast between the object of interest and the background or "noise."

CAMERAS

On Mission #140 the multispectral photographic data was recorded by the four camera Chicago Aerial KA62 system. The cameras have 12.7 cm x 12.7 cm format, a 7.6 cm focal length and use F/4.5 Paxar lenses. The system has vacuum platens, intralens shutters and minimum time of one second. The spatial resolution characteristics are listed in Table 4.

Table 4. Spatial resolution characteristics of the Chicago Aerial KA62 Cameras.

Altitude (m)	Ground Resolved Distance (m)
1000	.35*
3000	1.05*
10,000	3.5*
20,000	7.0*

*maximum contrast

FILM AND FILTER TYPES

Black and White Film

The film type referred to as B & W in later portions of this paper

is Plus X black and white film. The sensitivity versus wavelength of a typical B & W film is shown in Figure 17.

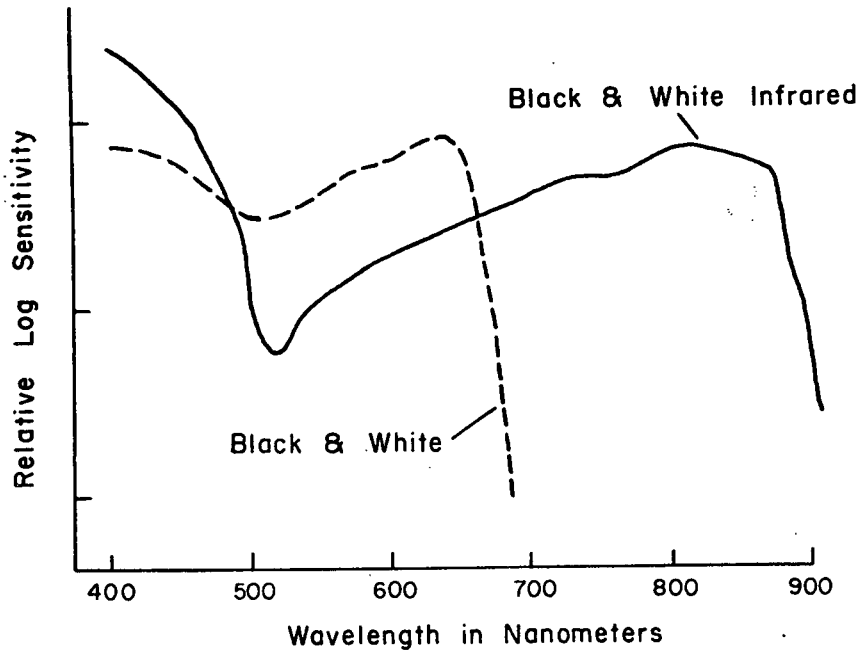

Figure 17 Spectral sensitivity of typical black and white and black and white infrared films.

The sensitivity of this film quickly drops above 700 nanometers, an important fact when selecting film filter combinations in multispectral experiments.

Black and White Infrared Film

This film referred to as black and white IR is sensitive both in the visible and near infrared portion of the spectra. Figure 17 also shows the curves of black and white infrared film sensitivity versus wavelength from 500 to 900 nanometers. Although this infrared film is sensitive to light at wavelengths shorter than 500 nanometers, this short wavelength sensitivity is normally blocked with an appropriate filter.

Since the human eye is not very sensitive above 725 nanometers, the black and white infrared film extends the target identification capability into an unseen portion of the spectrum. Because of this fact, a near infrared spectrometer becomes very useful in selecting the proper filters to be used with this type of film.

Filters

Two cameras in the cluster were loaded with black and white Plus X film and these cameras were filtered with a Wratten 58 (green) and Wratten 29 (red). The spectral transmission of these filters are shown in Figure 18. The third camera was loaded with black and white infrared film and filtered with a Wratten 87B filter (Figure 19).

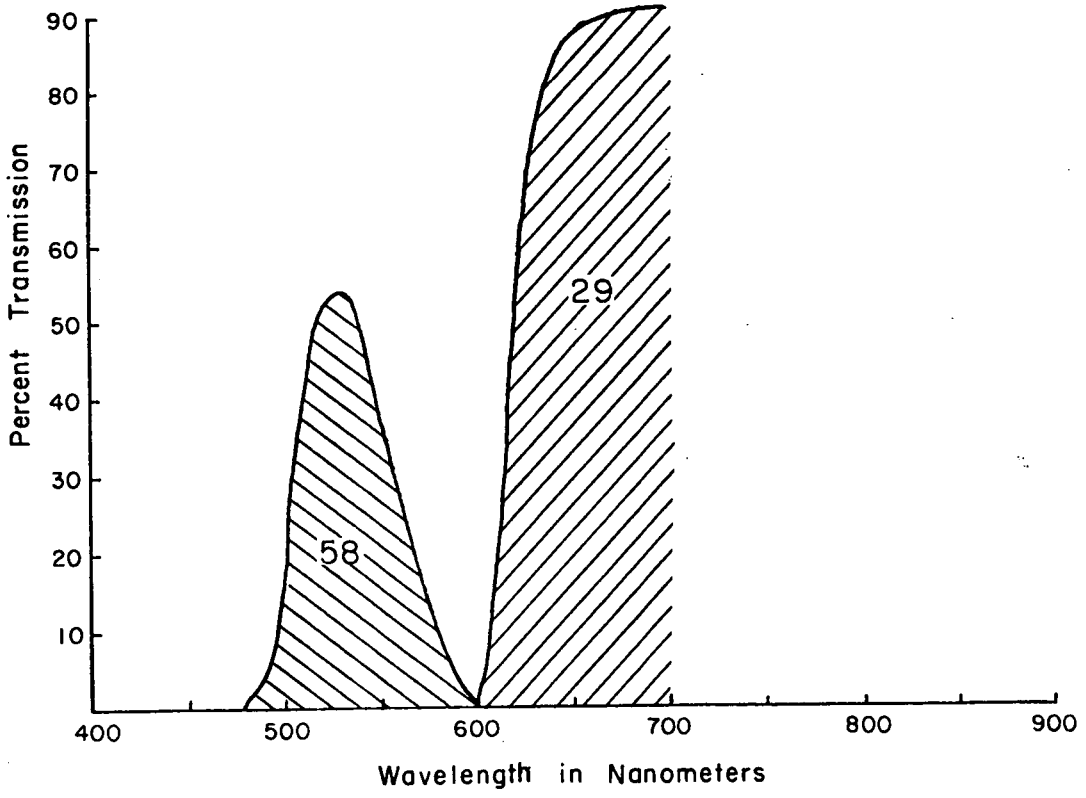

Figure 18 Transmission of Wratten No. 29 and No. 58 Filters.

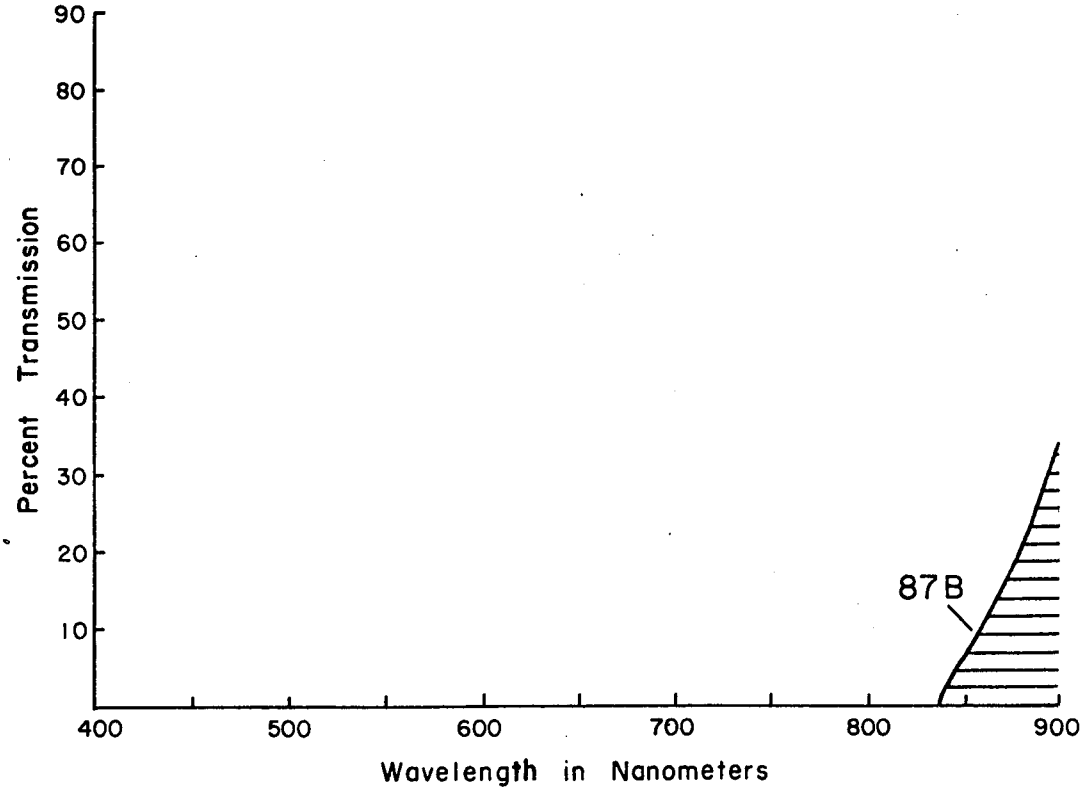

Figure 19 Transmission of Wratten No. 87B Filter

SPECTRAL REFLECTANCE MEASUREMENTS

The spectral reflectance characteristic of each of the rock types at Klondike Hills were measured with an ISCO Model SR spectroradiometer. This instrument measures the energy intensity (flux density) of incident light. Basically, the ISCO consists of a diffusing screen, light chopper, monochrometer, photo detector, amplifier and indicating meter.

Data Collection

Since albedo is a ratio of reflected radiation to incoming radiation, two separate measurements, solar energy flux and reflected radiation flux, are involved. The reflected radiation is best measured using the ISCO spectroradiometer with a remote fiber optics head (90^{o} field of view)

placed 7 to 15 cm above the target. The incoming radiation, for conformity, is also measured using the fiber optics head. To obtain incoming radiation the optics head is simply rotated 180°.

Numerically the spectral albedo is obtained by:

$$\text{Spectral albedo } (a_\lambda) = \frac{\text{reflected intensity } (R_\lambda)}{\text{incident intensity } (I_\lambda)}$$

Because albedo is the ratio of the instrument readings, none of the measurements need to be corrected for imperfect instrument transmission.

The most meaningful way in which this data can be presented is as a graph plotting albedo (reflectivity) against wavelength.

Figure 20 shows the spectral reflectance of select rock types from the Klondike Hills area together with the band pass limits of the filters used on the multispectral camera. These data will be referred to and described in detail in the section on data interpretation.

Preflight spectral reflectance data is invaluable for intelligent selection of film-filter combinations in multispectral photographic missions.

MULTISPECTRAL DATA INTERPRETATION

By referring to Figure 20, selected spectral reflectance curves of Klondike rock types, the following can be noted:

1. The Ge_4, Ge_2 and Opc units all have the same shaped optical reflectance curves and are only separable by slight differences in overall reflectance (albedo). These units would all appear dark gray to black on

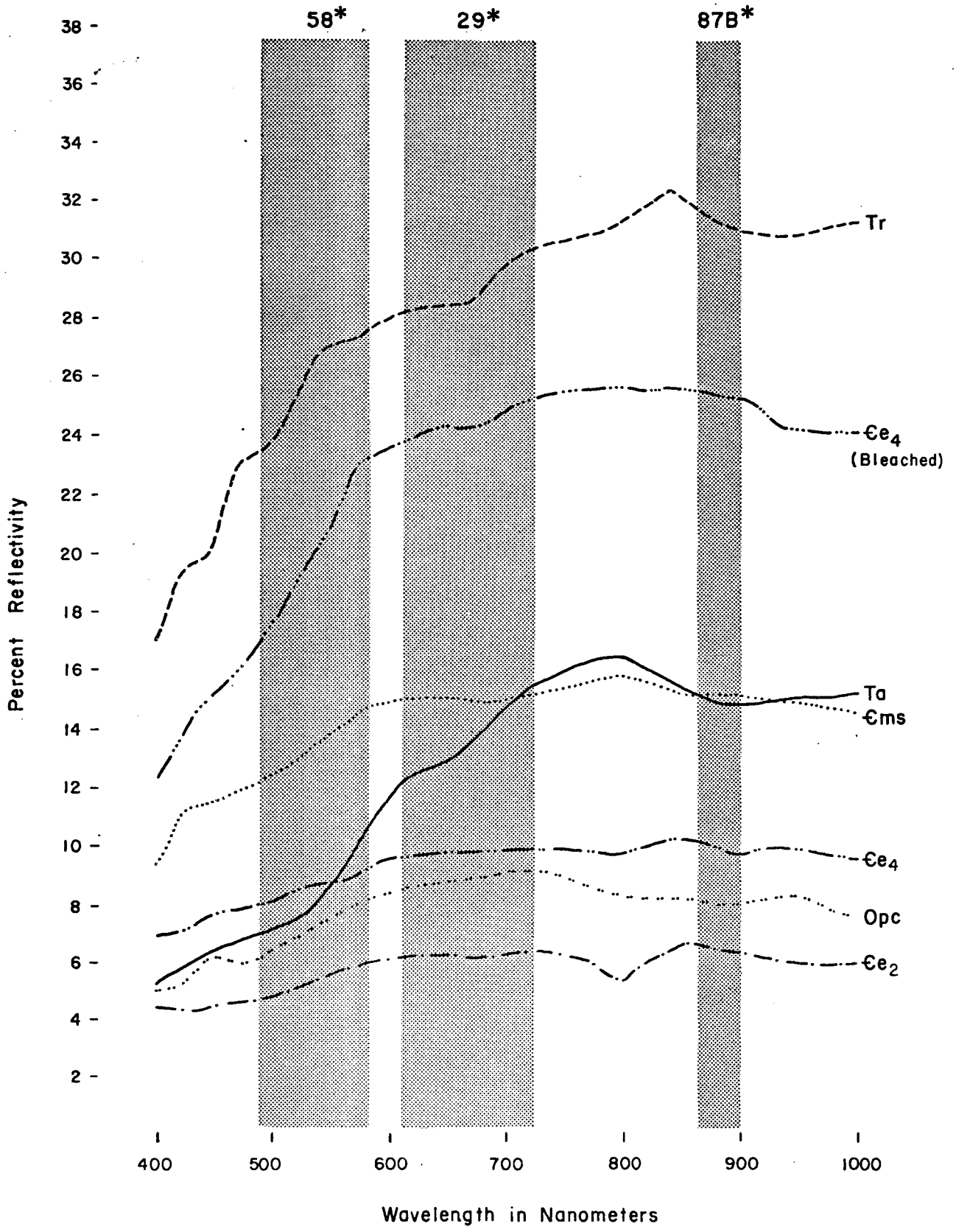

Figure 20 Selected spectral reflectance curves of rock types, Klondike Mining District, Nevada.

Page - 49

*Filters used in Mission No. 140 multispectral experiment

conventional B & W aerial photography and could only be delineated on over-exposed film.

2. The Gms, Ge_4 (bleached member) and the rhyolite (Tr) have generally higher total reflectivity than group one rocks. The reflectance in the green (58) is lower and the reflectivity in the near infrared is generally slightly higher than that of the red (29).

3. The andesite unit (Ta) has a distinctive shaped reflectance curve which is extremely low in the green portion of the spectrum and fairly high in the red and near infrared portion of the spectrum. Rock units with this type of "cross over" to the reflectance curve (with respect to the other units) are generally easy to differentiate with multispectral photography.

Figures 21, 22 and 23 show single frames from the KA62 over the northern portion of the Klondike district. When used in conjunction with Figure 24, the detailed geologic map of the northern portion of the district, several distinct points as to the reflectivity of the major rock units can be observed:

1. The Ge_4 and Ge_2 and Opc units are the consistently dark units in each of the multispectral photographs.

2. The Gms unit is intermediate in contrast in each photograph.

3. The Ta (andesite) unit is very dark in the green (58) photograph and intermediate in the other two photographs.

Many of the tonal differences described above would be lost or blended in conventional B & W areal photography. These differences in density on the film can be enhanced by a technique called masking.

Figure 21. Single frame of the KA62 camera loaded with B & W film and filtered with a Wratten 58 (green) filter.

Figure 22. Identical frame from KA62, filtered with a Wratten 29 filter (red).

Figure 23. Identical frame as in Figs. 21 and 22 from KA62 with near infrared film and Wratten 87B filter.

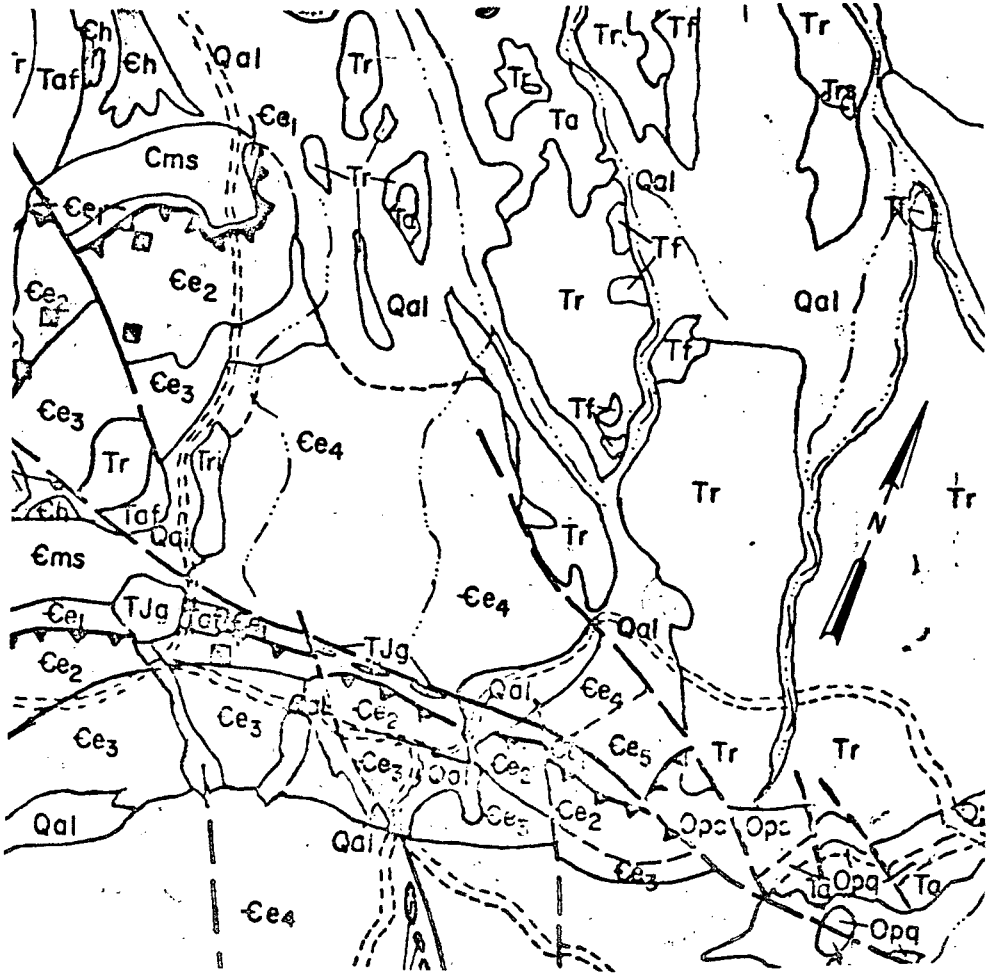

Figure 24. Detailed geologic map of the northern portion of the Klondike mining district.

A negative of the film taken from one portion (film-filter combination) of the multispectral camera and a transparent positive film from another different portion (film-filter combination) are transposed and a photographic print made of the composite. Figures 25 and 26 are examples of photographic masking to enhance features which are only subtly visible on single color negatives.

Figure 25 (a positive transparency from the green filtered camera (58) masked with a negative from the near infrared camera) enhances the differences in the rhyolite unit not normally detectable with B & W and/or conventional photography. Also the contrast between the rhyolite and the Quaternary alluvium is increased by this masking technique.

The mottled areas on the masked photographs are caused by slight registration problems and are mostly areas with high surface roughness (high shadow densities). Figure 26 shows a high contrast between the Ordovician chert unit and the volcanic and limestone units. This print was produced by masking a positive transparency from the green filtered camera and a negative from the red filtered camera. Folding and faulting in the Ge_4 unit on the upper right hand corner of the photograph is quite accentuated by the contrast between submembers of that limestone.

Reconstituted color photography produced from the three B & W films of the KA62 is the next step to refining the multispectral data. An infinite number of combinations of colors and color densities can be produced to supply to user with photography to meet his exacting needs of target identification. Figures 27 and 28 are two such reconstituted color photographs of the multispectral data over the Klondike district.

Figure 25. A print of the center of the Klondike district made by masking the film from the blue filtered camera (positive transparency) and a negative from the near infrared camera (87B).

Figure 26. A print of the same area made by masking a positive transparency from the green filtered camera and a negative from the red filtered camera.

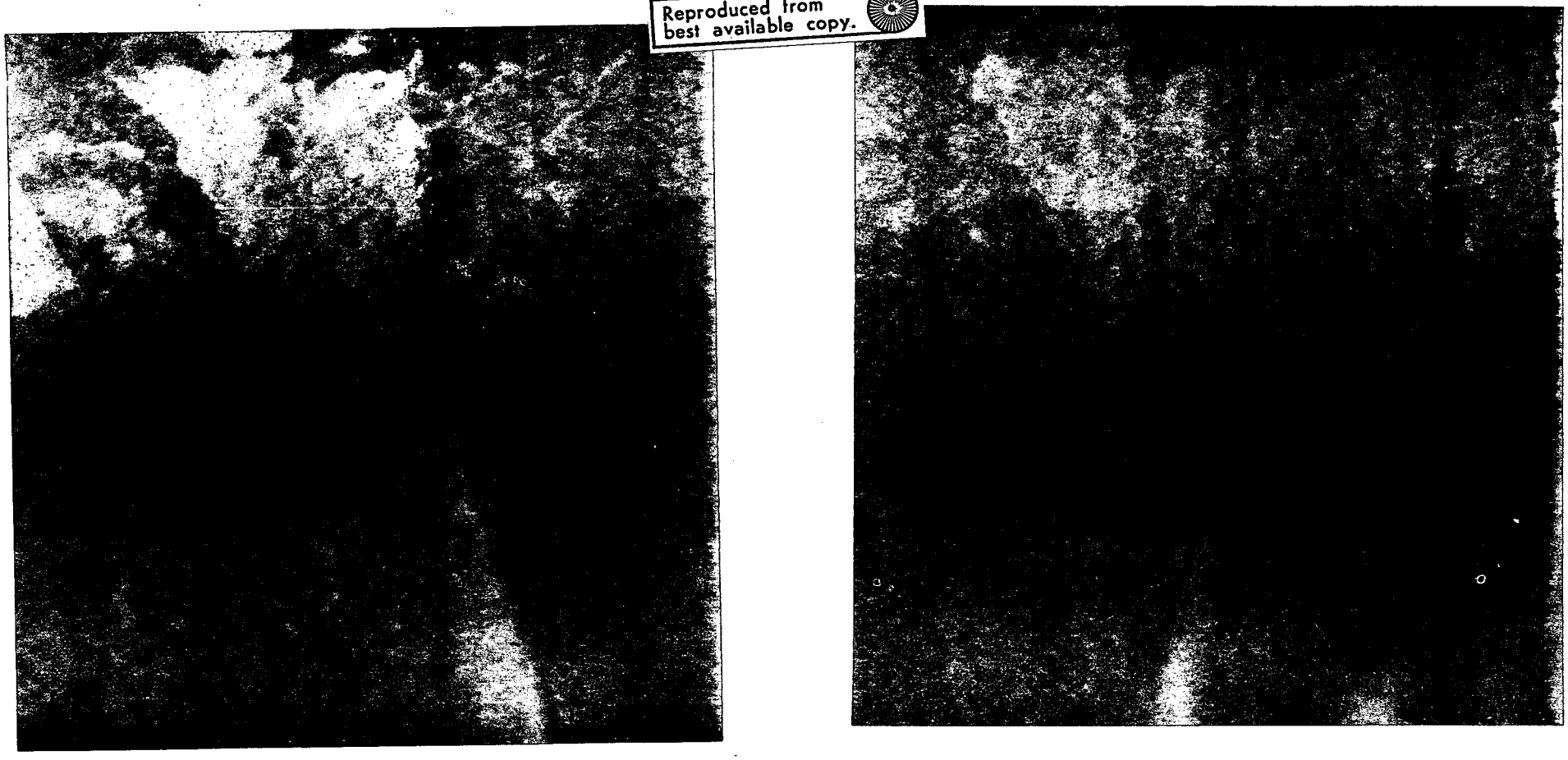

Figures 27 and 28. Reconstituted color photography of the central Klondike mining district.

They were produced using red (25), green (58) and blue (47) filtered light sources and varying the individual intensities of the light. The three transparencies were then brought into register on a photographic screen and the light intensities of each projector were varied to produce desired effects. Color photographic paper can be substituted for the screen if a permanent record of the reconstituted image is desired.

PHYSICAL FACTORS AFFECTING INFRARED

The tones on thermal infrared imagery, i.e., the apparent infrared radiometric temperature of the target, are controlled by three physical parameters: (1) the albedo, (2) the thermal diffusivity, and (3) the infrared emissivity.

Albedo

The albedo (reflectivity) is the reciprocal function of the solar energy available to the rock for heating.

$$(1-\alpha) = hr \qquad (1)$$

where α = reflectivity

h = solar energy available as heat

r = solar radiation flux

The variation in albedo of a particular rock or soil may be caused by differential surface mineralogy, an example of which is iron staining. Albedo variations with time may be caused by surface mositure which lowers the albedo (raises the energy available for heating). Total reflectivity (albedo) may be measured by integrating the area under the spectral albedo (reflectivity curves obtained in setting up photographic experiments) or may be obtained directly by use of a net radiometer.

Since albedo data is independent of incoming solar energy, solar radiation flux must be measured at the time of overflight to determine total heating. The solar radiation flux may be determined using a simple calibrated solar cell or by integrating the area under a spectrometer curve with the spectrometer pointed skyward.

Thermal Diffusivity

The thermal diffusivity is probably the most important physical parameter affecting the infrared temperature. It influences the transfer and storage of heat received from the sun. The thermal diffusivity may be influenced by pore water, alteration, cementation in particulate material and density.

In the laboratory, thermal diffusivity may be measured directly. The thermal diffusivity instrument has a transistor heated base plate which remains at a constant temperature as in a proportional oven. A precut core 12.0 mm in diameter and 25.0 mm in length is placed on the base plate, and a thermistor monitors the temperature at the opposite end of the core.

The thermal diffusivity is inversely proportional to the time taken by the unheated end of the core to rise some increment of temperature, if that increment is small with respect to the temperature difference between the base plate and the initial core temperature. The thermal diffusivity may be calculated by:

$$\kappa = \frac{C}{t} \qquad (2)$$

where κ = thermal diffusivity

t = time taken for incremental temperature rise

C* = an instrument constant

---

*"C" is not truly a constant dependent upon instrument design. The room temperature and base plate temperature of the instrument are also variables. For this reason the diffusivity chamber is best used with a stable power source in a "constant temperature" room.

To compensate for heat losses to the instrument and to the air, the instrument is calibrated using cores cut from standard materials. Those standard materials have been cut from oriented single crystals of quartz, calcite and fluorite.

The thermal diffusivity, κ, is equal to

$$\kappa = \frac{K}{c\rho} \qquad (3)$$

where K = thermal conductivity

κ = thermal diffusivity

c = specific heat

ρ = density

The thermal diffusivity of soils and other particulate matter may also be run in the diffusivity instrument. A styrofoam block with a hole the same dimensions as the rock cores is used as a container. A thin sheet of brass foil has been cemented to the base of the styrofoam holder. During operation the brass foil is heat sunk to the base plate of the diffusivity chamber, and the thermistor probe is placed directly in contact with the top of the cylinder of material, just as it is with solid rock cores.

Because thermal conductivity is largely a function of internal geometry of a material (i.e., the extent, type and preservation of grain boundaries), it may be useful to calculate thermal conductivity using formula (3) when specific heat and density are known. Since the rock and soil cores are of a standard size, their density may be determined by weighing each and dividing by their volumn (2.83 cm^3). The specific heat of most rocks is approximately .20; a better approximation may be

made using Kopp's Rule, if the elemental composition of the sample is known.

Infrared Emissivity

The third physical factor influencing the infrared radiometric temperature is the infrared emissivity. The emissivity is not as important as either diffusivity or albedo because the emissivity values for most rocks are confined to a fairly narrow range. The emissivity controls the balance of IR energy emitted which is characteristic of the rock's temperature and the energy emitted which is characteristic of the rock's surface. Emissivity is the decimal fraction of the emitted infrared energy characteristic of the target temperature. Since infrared radiation from opaque materials in the infrared can only result from the emissive and reflective components, their sum is 1.0.

$$\epsilon + \rho = 1 \qquad (4)$$

where ϵ = emissivity

ρ = reflectivity

Emitted radiation by a body is known to vary with temperature, composition and surface geometry. Surface geometry is a function of angularity, bump amplitude and distribution, as well as plane distribution, and is one of the major factors which control the heating, cooling and emitting characteristic of a given surface.

In the "water vapor" window (8-14 μm) of the infrared spectrum, emitted radiance can be approximated with the use of a constant temperature emissivity chamber. This instrument consists of a light-weight

portable radiation thermometer attached to a chamber which is capable of subjecting a change of temperature on a target surface.

A Barnes PRT-4 Radiation Thermometer is mounted on top of the emissivity chamber, which is constructed in such a fashion as to duplicate infinite parallel planes, where the lower surface is the target surface and the upper surface is of known temperature and emissivity. The upper surface of the chamber is so constructed as to be easily changed from one that is quite close to a blackbody [aluminum lid coated with 3M Covinal black (emissivity of approximately 0.98)] to a very highly reflecting surface [gold plated surface mirror (emissivity of approximately 0.02)]. The temperature of the blacked lid is maintained at a higher temperature from that of the surface under investigation. Thus, the greater the reflectivity of the target the greater is the difference of the two readings (when the mirror represents the upper surface and when the coated aluminum represents the upper surface). The numerical emissivity may be determined by calibration with known standards or by using a radiant power equation.

Combined Effects of Physical Parameters

If IR imagery is flown day-night the thermal effects of the thermal diffusivity and the albedo may be different. Because differening albedos have a marked effect on temperatures only during the day, the following scheme may be used to differentiate their effects:

	DAY				NIGHT			
		Thermal Diffusivity				Thermal Diffusivity		
		High	Low			High	Low
Albedo	High	cool	med	Albedo	High	warm	cold
	Low	med	hot		Low	warm	cold

The ground based radiometric measurements essentially duplicate the airborne infrared experiments. Radiometric temperatures taken at the times of overflights are proportional to the tones on the imagery (neglecting differential atmospheric attenuation). These radiometric temperatures provide a way of absolutely calibrating the thermal imagery (correlation of a specific film emulsion density to a given temperature) and ascertaining the weighted effect of albedo, then diffusivity and emissivity on the various targets. The rational for measuring the albedo, emissivity and thermal diffusivity is that the specific physical attributes such as moisture, density, alteration, etc., causing the thermal anomaly, cannot be deduced from radiometric temperature measurements alone.

GROUND TRUTH FOR THE INFRARED

Four types of ground truth data have been collected in the Klondike Mining District which aid in the evaluation and interpretation of the infrared imagery. Prior to the flight, thermal diffusivity and albedo measurements were made on a number of the rock units (Table 5). During the flight, infrared radiometric temperatures and solar radiation flux were measured (Table 6 and Figure 29).

In addition to being able to place absolute temperatures on the infrared imagery, the ground based infrared radiometric temperatures

Table 5. Physical Parameters of Rocks.

Rock Unit		Thermal Diffusivity (κ)	Albedo (α)
Gh	limestone	.0191	--
Gms	limestone	--	.14
Ge_1	argillite	.0111-.0154	.22
Ge_2	argillaceous limestone	.0166	.05
Ge_3	siltstone	.0120	.09
Ge_4	limestone	.0181	.08
Ge_5	banded argillite	--	.11
Opc-Opl	cherty limestone	.0177	.08
Opq	quartzite	.0255	.08
KJg	Granite	.0201	.21
Tr	rhyolite	.0117	.27
Trs	silicified rhyolite	.0198	.27
Ta	andesite	.0129-.0142	.12
Tb	basalt	.0117	--
Taf	ash flow tuff	.0156	--

Table 6. Ground Based Infrared Radiometric Temperatures.

Unit	Day Temp (12:00) outcrop	talus	Night Temp (4:00) outcrop	talus
Ge_4 (bleached)	34°	36°	18°	14°
Ge_4 (dark)	40° cloud	38°	17°	15°
Ge_4 (dark)	40°	--	18°	--
Ge_4 (med)	36°	--	20°	--
Ge_5	--	50°	--	16°
Opl	48°	51°	20°	17°
Opc-Opl	46°	51°	20°	17°
Tr	34°	--	15°	--

provide a method for checking the albedo, thermal diffusivity and solar radiation flux data. In the daytime data, in each case except one, the broken rock or talus is warmer than the rock outcrop. This illustrates the effect of thermal diffusivity on the daytime data; as the albedo and emissivity are the same and only the thermal diffusivity is lower in the talus. The nighttime data for the same units show just the reverse, for

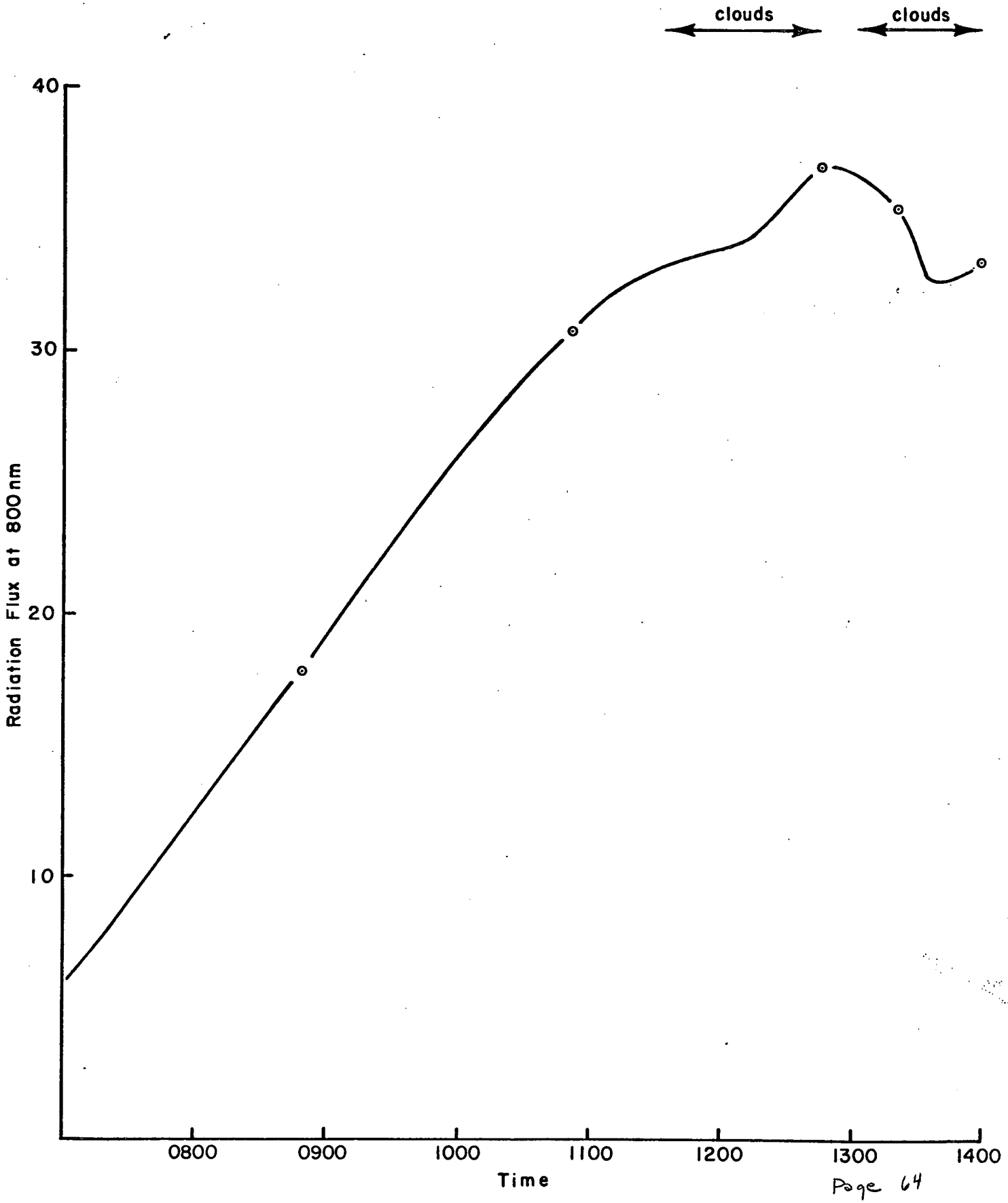

Page 64

Figure 29 Solar intensity curve August 15, 1970

the heat rapidly transmitted to depth during the day is reconducted to the surface to make the outcrops warmer at night. The single exception on the daytime data corresponds to the time in which a cloud drifted over. This situation mimics the nighttime case in which rocks with high thermal diffusivity begin to transmit heat back to the surface, keeping their temperatures nearly the same while the low diffusivity materials cool off rapidly.

Table 6 also illustrates the effects of differing albedos on the temperature of rocks and soils. The Ge_4 unit whose temperature was measured in four localities has about the same thermal diffusivity and infrared emissivity from place to place. Its color and albedo do, however, vary, giving rise to quite different daytime temperatures, the lighter colored units being cooler due to their higher albedos.

Data from Figure 29, the solar intensity curve, when combined with the albedo is primarily useful in comparing data taken at different times during a day or on different days. The greater the solar intensity the greater the temperature spread due to both albedo and thermal diffusivity.

EVALUATION OF THERMAL INFRARED IMAGERY

A Texas Instruments RS-14 infrared imager operating at 8-14μm was used to obtain day and night thermal imagery. The 1000 m flight elevation resulted in 70mm imagery with an initial scale of approximately 1:20,000. Prints of both the day and night imagery of the northern end of the flight line are shown in figure 30.

In the sections of text above, it has been shown that the various rock units on the site have differing albedos and thermal diffusivities, and thus have different infrared temperatures. On the basis of this, it is possible to map certain rocks on the infrared imagery. Table 7 lists these rock units which have distinct tones on the pre-dawn infrared imagery. The first units noted are the warmest, the last the coldest. To the right is listed the thermal diffusivities which have dominent control of the nocturnal temperatures. Table 8 lists those rock units which appear distinct on the mid-day thermal imagery. The hottest units are listed first and both the thermal diffusivity and albedo of each are given at the right. Because the relative contribution of thermal diffusivity and albedo is not fixed, but is dependent upon the solar radiation flux, air temperature, sky temperature and several other variables, only a few generalities may be made about which units are differentiable on the mid-day imagery. In general these rocks with low albedo and low thermal diffusivity will appear hottest and those with high albedo and high thermal diffusivity the coolest.

PREDAWN

White is warm - Black is cold

Figure 30 Thermal infrared imagery - North half Klondike Mining District

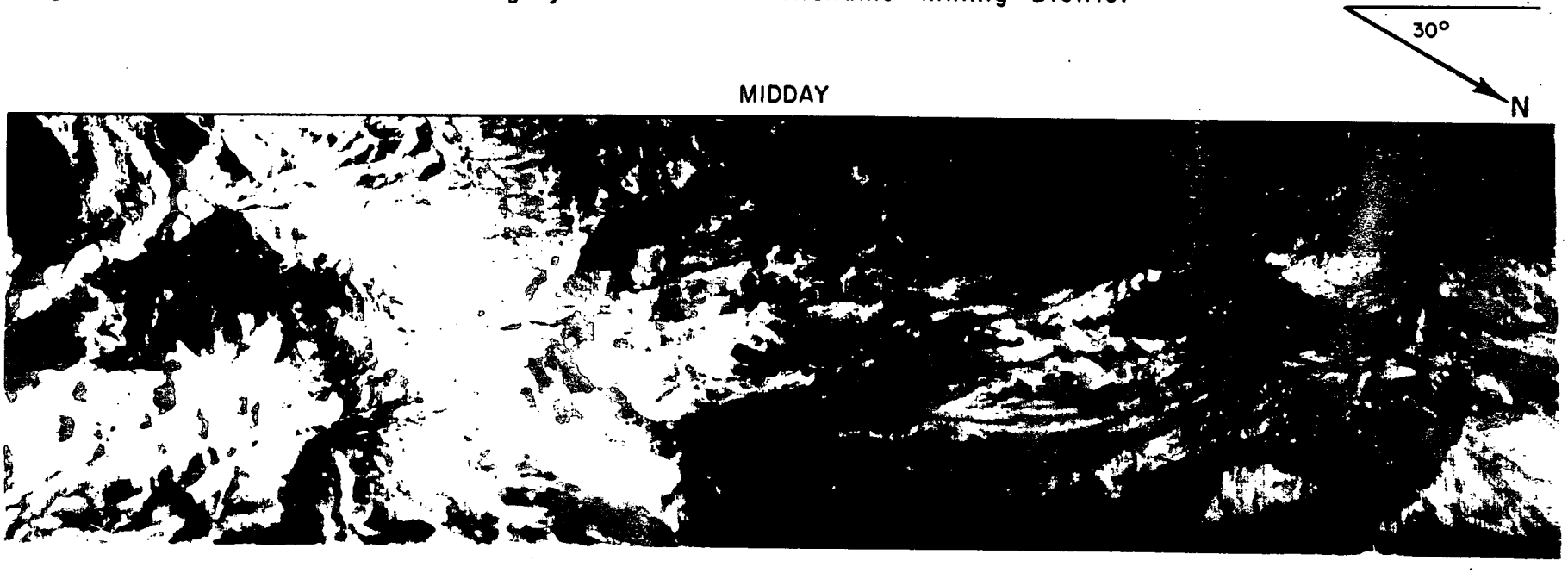

L9

Table 7. Night Relative Radiometric Temperatures of Geologic Units.

	Unit	Thermal Diffusivity (κ)
Warm	Opq	.0255
↑	Trs	.0198
	Ge_4	.0181
	Ge_2	.0166
	various ls & argillites	.0120-.0160
	Tf	~.0125*
	Qal	~.0080-.0120*
Cold	Tr	.0117

*Estimate from similar rock in other areas. Not actually measured.

Table 8. Day Relative Radiometric Temperatures of Geologic Units.

	Unit	Thermal Diffusivity (κ)	Albedo (α)
Hot	Ta	.0135	.12
↑	Ge_4 (bleached)	.0181	~.20*
	various ls & argillites	.0120-.0160	.05-.11
	Tf	~.0125*	~.25*
	Qal	~.0080-.0120*	~.10*
	Tr	.0117	.27
Cool	Trs	.0198	.27

*Estimate from similar rock in other areas. Not actually measured.

Each of the rock units listed in Tables 7 and 8 may be differentiated and mapped on the thermal imagery shown in Figure 30. Numerous other units may also be mapped because they lie stratigraphically between rocks with differing thermal characteristics, even though they may not be uniquely identified. A number of lineations and faults may also be seen on the imagery, for direct comparison with mapped structures (see Plate 1, pocket). A selected area of thermal infrared imagery blown up to the approximate map scale used in mapping the mining district (1:12,000) show considerable geologic detail.

The 8-14μm thermal imagery (somewhat distorted) and matching geologic map are shown in Figures 31 and 32. The warmest unit on the night thermal imagery shown is an "infrared marker horizon" within the Ge_2 unit. This marker bed was discovered on this thermal imagery. It consists of a dense quartzite which is undistinguishable from the remainder of the Ge_2 unit on areal photography. Table 9 identifies the geologic units according to their tones on the imagery.

Table 9. Relative temperatures of rock units appearing in Figures 31 and 32.

Rock	Tone	Temperature
Ge_2 (marker) Ge_4 (silicified along major faults) Gms Ge_2 Ge_4 Tb Qal Ge_1 Qal Tr Qal	White ↕ Black	Warm ↕ Cold

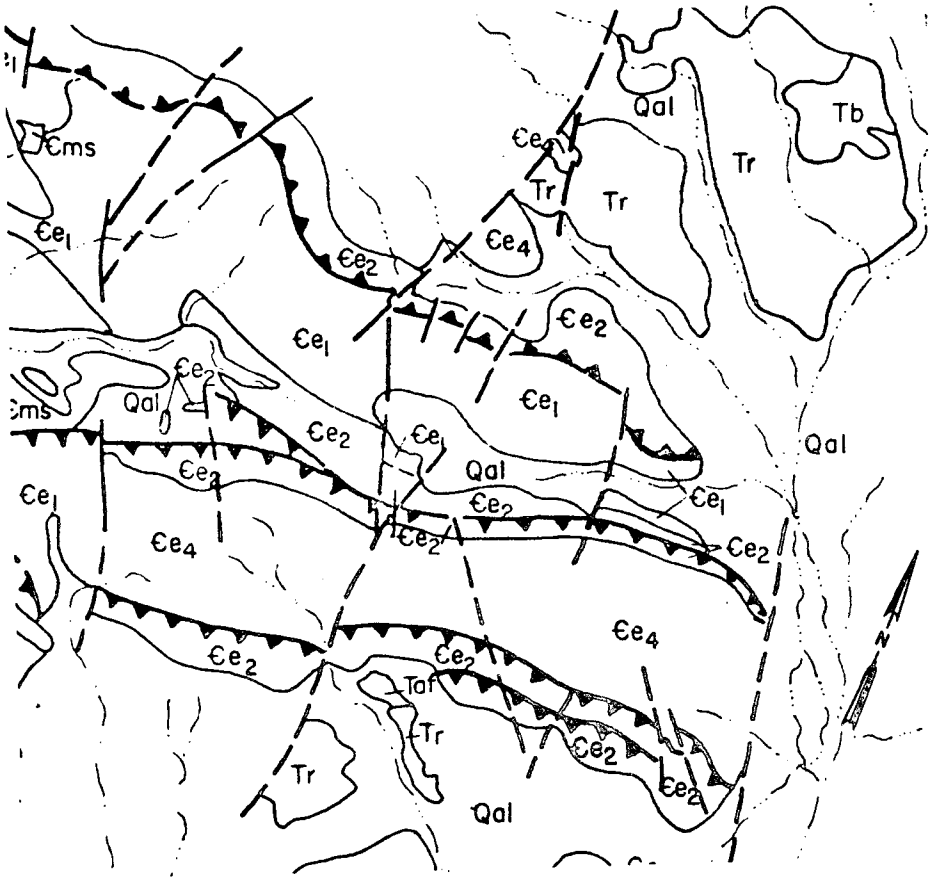

Figure 31. Geologic map of thrusted limestone area south end of Klondike Mining District.

Figure 32. Pre-dawn thermal imagery of thrusted limestone area, south end of Klondike Mining District.

The geologic mapping of the area is in general excellent. It shows all of those features which can be seen on areal photography and confirmed on the ground, as well as many features not discernable on air photos. In the south area shown in Figures 31 and 32, numerous features unidentifiable on the air photography, and not apparent on the ground, may be seen on the thermal imagery. Corrections and additions to the geologic mapping are as follows:

(a) Ge_2 marker horizon is repeated perhaps in a small thrust slice or low angle normal fault.

(b) Ge_2 marker horizon cut by a small north-south trending fault not shown.

(c) The fault shown at (c) is of considerably greater extent than shown, continuing north across the Tr to point (C').

(d) An unmapped fault extending from (d) to (d') cuts Ge_2.

(e) The fault shown at (e) extends northward across the Qal and the Gms units, presumably to connect to the fault shown at e'.

Figure 33 shows a geologic map corrected solely from infrared imagery.

Figures 34, 35 and 36 are matching day and night thermal imagery and geologic map of a portion of the north end of the flight line. This area is also shown on the color photograph (Figure 13). In this volcanic area it may be seen that the volcanic units are much less homogeneous than the sedimentary units. The Ta (andesite) and Trs (silicified rhyolite) units are very distinct. The Tr and Taf (rhyolite and rhyolitic welded ash flow tuffs) units are laterally gradational. The Qal (alluvium) is

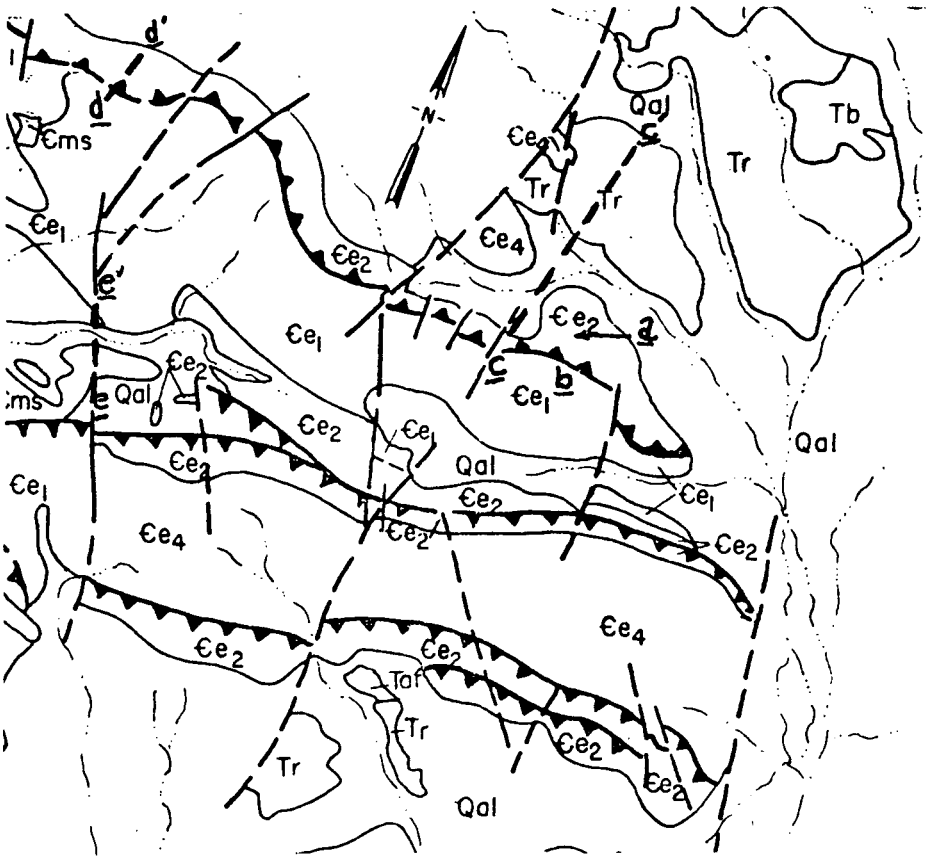

Figure 33. Geologic map revised from thermal imagery, thrusted limestone area, Klondike Mining District.

Figure 34. Mid-day thermal imagery, volcanic area, north end, Klondike Mining District.

Figure 35. Pre-dawn thermal imagery, volcanic area, north end, Klondike Mining District.

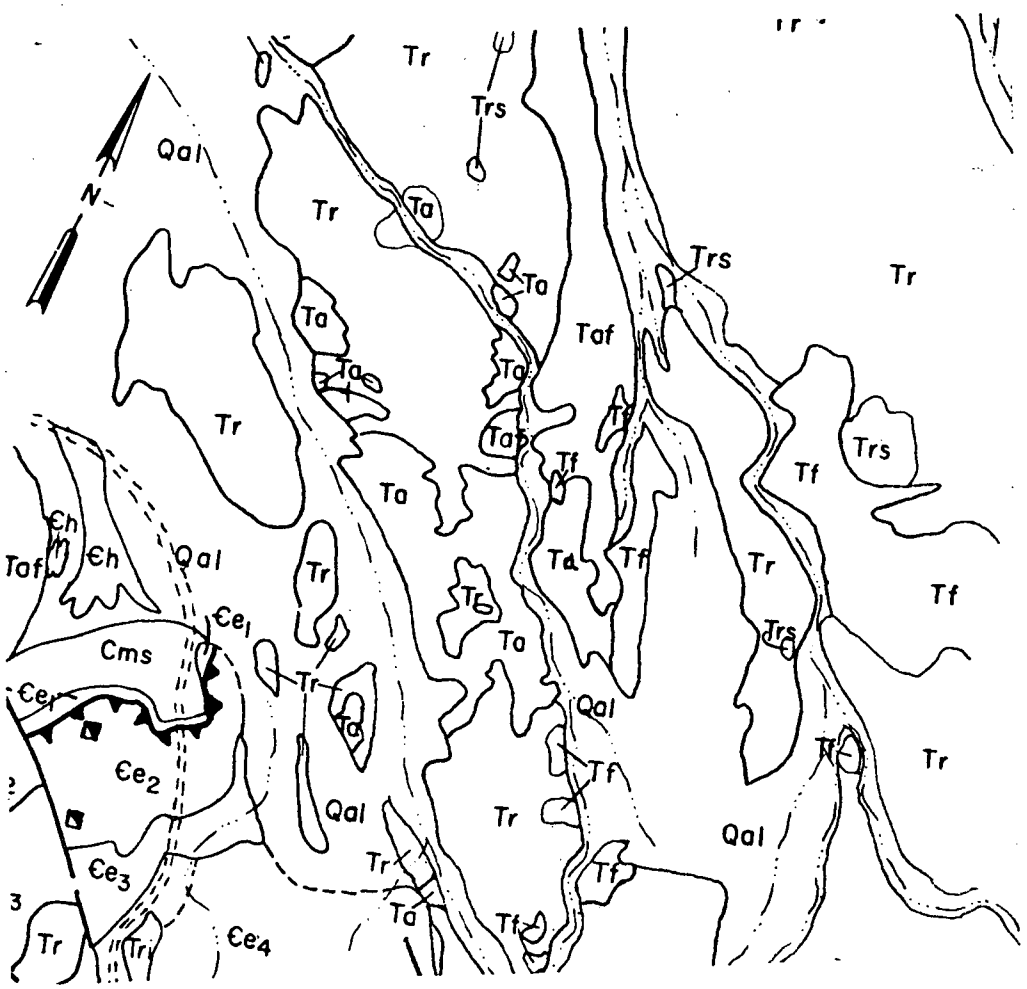

Figure 36. Geologic map, volcanic area, north end, Klondike Mining District.

very dependent upon the original rock material from which it is derived, hence, is rather irregular in temperature. Table 10 lists the characteristic temperatures of volcanic units as derived from the thermal imagery.

Table 10. Temperatures of units in the north volcanic area.

Unit	Day Temperature	Night Temperature
Ta (andesite)	Hot	Intermediate
Tf (tuff breccia)	Warm	Intermediate
Trs (silicified rhyolite)	Cool	Warm
Qal (alluvium)	Intermediate	Cold
Tr (rhyolite)	Warm to Cool	Intermediate to Cold

Of the units listed in Table 10 only those mapped as Tr appear to have no distinct thermal signature. This rhyolitic unit is not, however, continuously variable and may be subdivided into three distinct units. On the basis of the thermal characteristics of rhyolite to the south which is definitely intrusive, it is suggested that those rhyolites on the extreme western edge of the area shown in Figure 36 be included with the Tri subdivision. Most of the remaining rhyolite is obviously rhyolite flows which are adequately covered by the symbol Tr. The third proposed rhyolitic unit is exposed only on the northeast corner of the area shown in Figure 36. This unit has a higher daytime temperature than the other rhyolitic subdivision and a nighttime temperatire as low as the Tri. This indicated an albedo somewhat lower (darker color) than the other rhyolites and its thermal conductivity is approximately equal to that of the Tri (κ = .0117). Table 11 outlines the thermal responses of the three proposed rhyolitic units.

Table 11. Thermal responses of rhyolitic units.

Unit	Day Temperature	Night Temperature
Tri	Cool	Cold
Tr	Intermediate	Intermediate
Trd	Warm	Cold

When Trd and Tr are mapped separately, a long linear contact is created. This contact is aligned with several other minor linear structures and probably represents a fault. This relationship is best seen on the strip of imagery (Figure 30) which includes the entire northern half of the flight line. Figure 37 incorporates the above suggestions on a geologic map revised on the basis of the thermal imagery.

The pre-dawn thermal imagery and matching geologic map shown in Figures 38 and 39 is of the same region shown in the photographic and multispectral photographic sections (see Figures 16, 27 and 28). As in the pre-dawn imagery of other areas in the Klondike Mining District, the volcanics are coldest (darkest). Alluvium, shales and limestones are of intermediate temperatures, which the dense siliceous materials, quartzites, cherts and silicified limestones are the warmest. This thermal behavior may be predicted from the thermal diffusivities of the materials involved. Several features on this portion of the test site are more clearly visible on the thermal imagery than by any other method. They include the following:

(1) In the upper right corner of Figure 38 the shales and limestones are differentiated from the warmer quartzites. The white filamental characteristics are individual thin quartzite beds separated by shales.

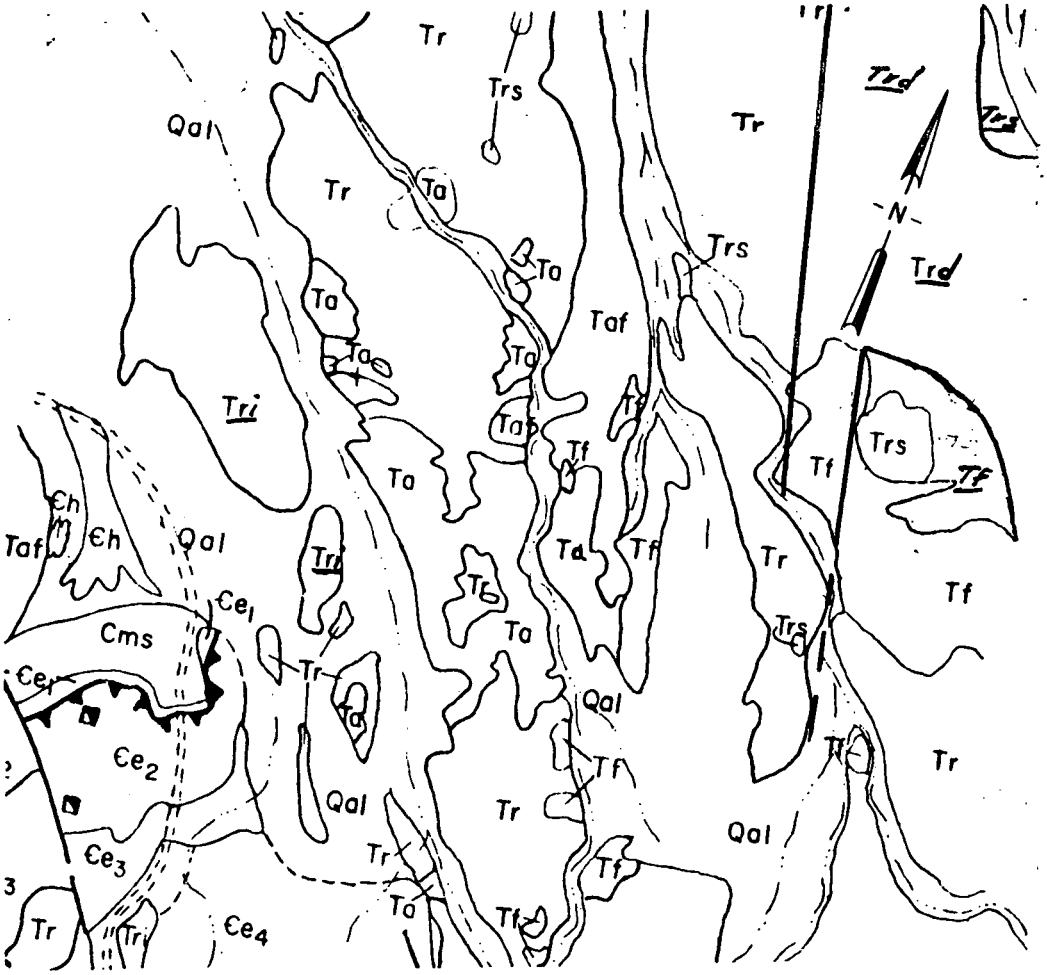

Figure 37. Geologic map revised from thermal imagery, volcanic area, Klondike Mining District.

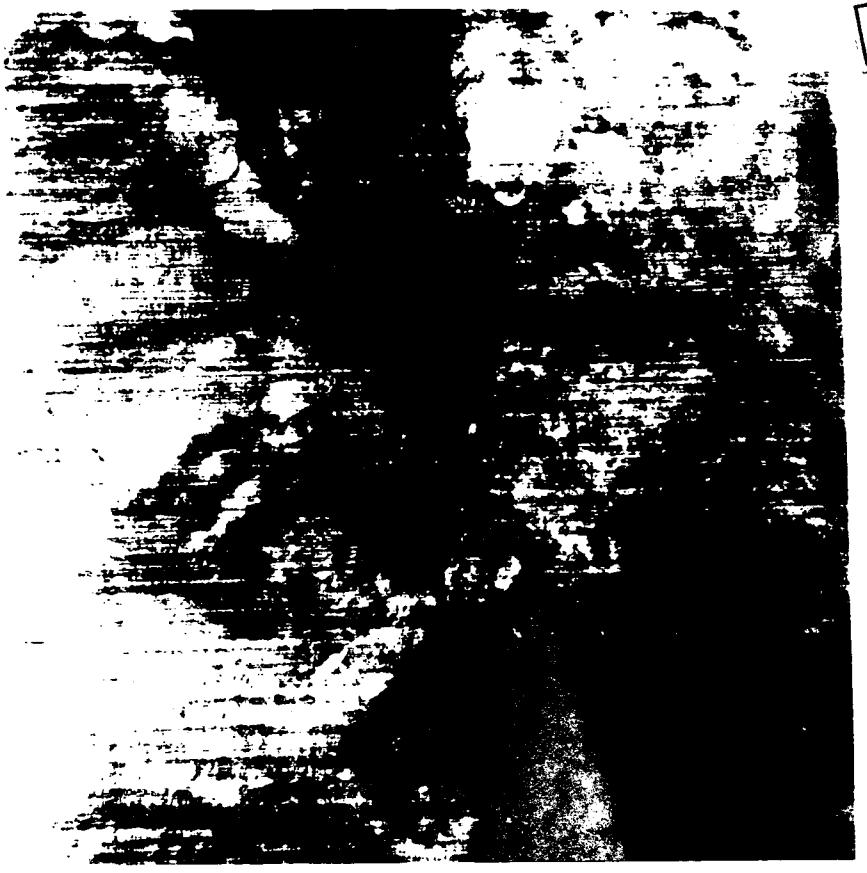

Figure 38. Pre-dawn thermal imagery of the central area of the test site.

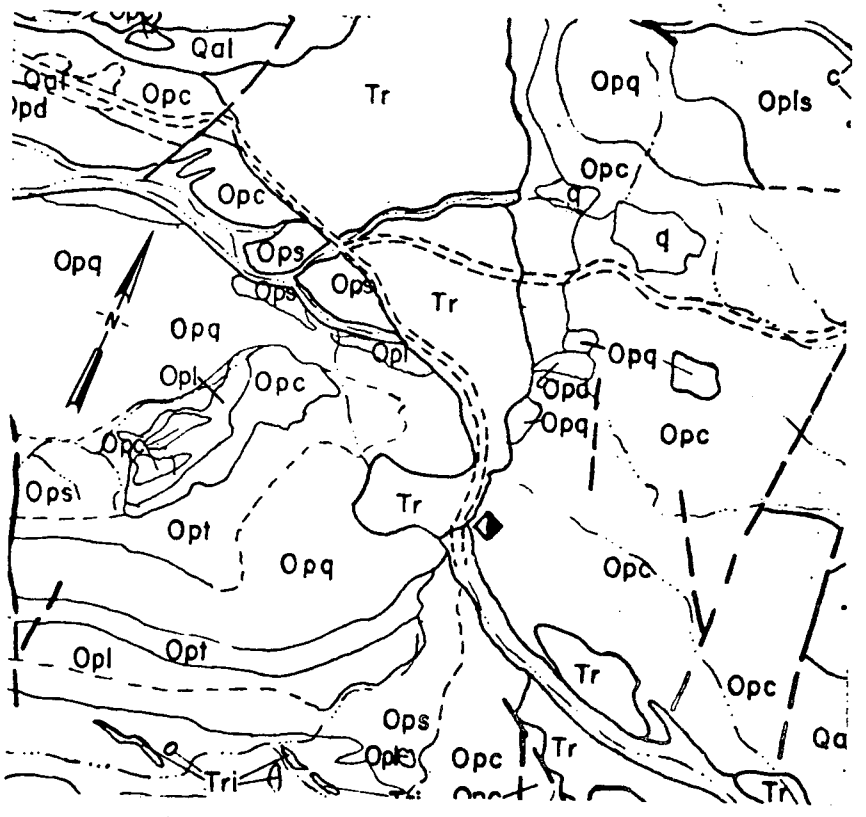

Figure 39. Geologic map of the central area of the test site.

It may be seen on the imagery that the area is highly disturbed with rather large sheets of quartzite resting at a variety of attitudes.

(2) An east-trending stream beginning almost at the center of Figure 38 is seen to be far more linear than it appears on photographs. Higher and lower diffusivity materials are oriented along the lineation; they are almost certainly silicified zones and rhyolite intrusions -- indications that the lineation is a fault.

(3) A lineation may be seen about 3 cm left of center oriented approximately N-S. This linear feature separates Ordovician shales from limestone and cherts and probably represents a fault.

(4) The large patch of rhyolite dominating the top of the image (Figure 38) tends to have areas of higher thermal diffusivity. This area follows the area differentiated well on the masked multispectral photography, and may, by its general appearance and configuration, indicate an area of thin volcanic cover.

As a final note to the interpretation of thermal imagery, it should be observed that anomalous daytime temperatures occur in shadows. Because of the differential weathering characteristics of certain rock units such as the Trs and the Opq, they are nearly always accompanied by such shadows and care must be taken not to interpret the shadows as a reflection of their true thermal characteristics.

CONCLUSIONS

The foregoing discussions demonstrate the usefulness of infrared imagery, not only in mapping but also in ascertaining some of the physical properties of rocks from the reconnaissance aircraft. Many of these physical attributes are not recognizable by albedo and color which are obtainable from areal photography. It should also be clear the albedo (reflectivity) may be more accurately measured from areal photographs, and that "ground truth" measurably enhances the usefulness of the infrared imagery. The evaluation of imagery has also shown that the effects of albedo, thermal diffusivity and infrared emissivity and their underlying geologic attributes may not be determined without day-night imagery. The following set of rules for the use of infrared imagery is hereby proposed from the results of this and previous infrared imagery experiments:

1. No infrared imagery should be obtained except under clear weather conditions. A period of at least two hours of cloudless conditions should preceed any daytime flights.
2. Matching areal photography, preferably both wide-latitude black and white and color, should be flown with day infrared imagery.
3. Matching day and night thermal imagery should be obtained (on successive half days if possible).
4. At least minimal "ground truth" (terrametric) information should be collected. It should include soil and surface moisture, radiometric temperatures, and samples of sufficient size to conduct later albedo, thermal diffusivity and infrared emissivity measurements if deemed necessary.

5. Air photography, thermal imagery, topographic base and previous mapping (if they exist) should be reduced to a common scale before evaluation is attempted.

REFERENCES CITED

Albers, John P., and Stewart, J.H., 1965, Preliminary geologic map of Esmeralda County, Nevada, 1:200,000: U.S. Geol. Surv. Mineral Inv., Field Map MF-298.

Brennan, P. A., 1968, Albedo Measurements at the Mt. Lassen Test Site: Univ. of Nevada NASA Technical Letter No. 16.

Buetner and Kern, 1965, The Determination of Infrared Emissivity of Terrestrial Surfaces: JGR, vol. 70, No. 6.

Chapman, P. E., 1966, Variations of Emissivity in the infrared range (8-14μ): Univ. of Nevada NASA Technical Letter No. 2.

Chapman, P.E., and P. A. Brennan, 1969, Ground Truth Acquisition: First International Remote Sensing Institute Symposium.

Chipp, E. R., 1969, Geology of the Klondike Mining District, Nevada: Unpub. M.S. Thesis, Univ. of Nevada.

Cornwall, Henry R., 1967, Preliminary geological map of southern Nye County, Nevada, 1:200,000: U.S. Geol. Surv. Open File Map No. 16.

Hewett, D. F., et. al., 1936, Mineral Resources of the region around Boulder Dam: U.S. Geol. Surv. Bull. 871.

Quade, J. G., P. E. Chapman, P. A. Brennan, and J. Blinn, 1970, Multispectral Remote Sensing of an Exposed Volcanic Province, Jet Propulsion Laboratory Technical Memorandum 33-453.

Vanderburg, W. O., 1936, Placer Mining in Nevada: Nevada Univ. Bull., v. 30, no. 4, p. 79.